Biochimica et Biophysica Acta 1820 (2012) 9–23

Contents lists available at SciVerse ScienceDirect

Biochimica et Biophysica Acta

journal homepage: www.elsevier.com/locate/bbagen

S-allyl cysteine in combination with clotrimazole downregulates Fas induced apoptotic events in erythrocytes of mice exposed to lead

Samir Mandal [a], Sudip Mukherjee [b], Kaustav Dutta Chowdhury [b], Avik Sarkar [a], Kankana Basu [b], Soumosish Paul [b], Debasish Karmakar [b], Mahasweta Chatterjee [b], Tuli Biswas [a], Gobinda Chandra Sadhukhan [b], Gargi Sen [a,*]

[a] Indian Institute of Chemical Biology (CSIR), 4, Raja S.C. Mullick Road, Kolkata-700032, India
[b] Department of Zoology, Vidyasagar College, 39 Sankar Ghosh Lane, Kolkata-700006, India

ARTICLE INFO

Article history:
Received 1 August 2011
Received in revised form 28 September 2011
Accepted 30 September 2011
Available online 14 October 2011

Keywords:
Lead
Erythrocyte
S allyl cysteine
Clotrimazole
Reactive oxygen species
Apoptosis

ABSTRACT

Background: Chronic lead (Pb^{2+}) exposure leads to the reduced lifespan of erythrocytes. Oxidative stress and K^+ loss accelerate Fas translocation into lipid raft microdomains inducing Fas mediated death signaling in these erythrocytes. Pathophysiological-based therapeutic strategies to combat against erythrocyte death were evaluated using garlic-derived organosulfur compounds like diallyl disulfide (DADS), S allyl cysteine (SAC) and imidazole based Gardos channel inhibitor clotrimazole (CLT).

Methods: Morphological alterations in erythrocytes were evaluated using scanning electron microscopy. Events associated with erythrocyte death were evaluated using radio labeled probes, flow cytometry and activity gel assay. Mass spectrometry was used for detection of GSH–4-hydroxy-*trans*-2-nonenal (HNE) adducts. Fas redistribution into the lipid rafts was studied using immunoblotting technique and confocal microscopy.

Results: Combination of SAC and CLT was better than DADS and CLT combination and monotherapy with these agents in prolonging the survival of erythrocytes during chronic Pb^{2+} exposure. Combination therapy with SAC and CLT prevented redistribution of Fas into the lipid rafts of the plasma membrane and downregulated Fas-dependent death events in erythrocytes of mice exposed to Pb^{2+}.

Conclusion and general significance: Ceramide generation was a critical component of Fas receptor-induced apoptosis, since inhibition of acid sphingomyelinase (aSMase) interfered with Fas-induced apoptosis during Pb^{2+} exposure. Combination therapy with SAC and CLT downregulated apoptotic events in erythrocytes by antagonizing oxidative stress and Gardos channel that led to suppression of ceramide-initiated Fas aggregation in lipid rafts. Hence, combination therapy with SAC and CLT may be a potential therapeutic option for enhancing the lifespan of erythrocytes during Pb^{2+} toxicity.

1. Introduction

Chronic Pb^{2+} toxicity is one of the most critical environmental health hazards affecting children and women [1,2]. The symptoms of Pb^{2+} toxicity include cognitive decline, hyperactivity, and anemia [2]. The exposure to Pb^{2+} can occur through inhalation or oral routes [3]. Once it enters the bloodstream, it is circulated throughout the body, giving rise to many pathological symptoms [2]. Erythrocytes are an early and primary target of Pb^{2+} induced toxicity after it reaches the systemic circulation [4]. Much of the Pb^{2+} in circulation gets accumulated and retained in erythrocytes [2]. The sequelae of events that occur during anemia associated with chronic Pb^{2+} exposure include premature elimination of circulating erythrocytes and ineffective erythropoiesis due to interference in heme biosynthesis [5]. Pb^{2+} ions get adhered to the external and internal surfaces of the erythrocyte membrane [6] causing disorder in lipid bilayer and conformational change in the membrane proteins [6]. Intracellular

Abbreviations: FITC, fluorescein isothiocyanate; PS, phosphatidylserine; Prx2, peroxiredoxin2; NAD, nicotinamide adenine dinucleotide; NADP, nicotinamide adenine dinucleotide phosphate; NADH, nicotinamide adenine dinucleotide reduced; NADPH, nicotinamide adenine dinucleotide phosphate reduced; HPF, 3′-(p-hydroxyphenyl) fluorescein; FACS, fluorescence-activated cell sorting; Pb^{2+}, lead; SAC, S allyl cysteine; CLT, clotrimazole; ROS, reactive oxygen species; $OH^{\bullet-}$, hydroxyl radical; GSH, glutathione; K^+, potassium ion; DMSA, meso-2, 3-dimercaptosuccinic acid; MiADMSA, monoisoamyl meso-2, 3-dimercaptosuccinic acid; DADS, diallyl disulfide; GST, glutathione S transferase; SGPT, serum glutamate pyruvate transaminase; SGOT, serum oxaloacetate transaminase; WBCs, white blood cells; RBCs, red blood cells; PBS, phosphate buffer saline; HNE, hydroxynonenal; TBARS, thiobarbituric acid reactive substance; TBA, thiobarbituric acid; DTNB, 5,5′-dithiobis-2-nitrobenzoic acid; CDNB, 1-cloro-2,4-dinitrobenzene; FCS, fetal calf serum; aSMase, acid sphingomyelinase; BSA, bovine serum albumin; DMTU, dimethyl thiourea; DAS, diallyl sulfide; LDL,, low-density lipoprotein; −SH group, sulfhydryl group; H_2O_2, hydrogen peroxide; GPx, glutathione peroxidase; DISC, death inducing signaling complex

* Corresponding author at: Indian Institute of Chemical Biology, CSIR, 4, Raja S.C. Mullick Road, Jadavpur, Kolkata-700032, India. Tel.: +91 33 2473 3491; fax: +91 33 2473 0284.
E-mail addresses: sengargi@hotmail.com, gargisen2010@gmail.com (G. Sen).

0304-4165/$ – see front matter © 2011 Elsevier B.V. All rights reserved.
doi:10.1016/j.bbagen.2011.09.019

accumulation of Pb^{2+} ions leads to metabolic starvation with concomitant decrease in the ATP generation [2]. ATP decrement is accompanied by loss of balance between ROS production and antioxidant systems in the intra-erythrocyte microenvironment [2,7]. Reports suggest that Pb^{2+} exposure exacerbates generation of OH^- in erythrocytes [2,7,8]. K^+ loss is also another important feature of the Pb^{2+} exposed erythrocytes [9]. Ion channels responsible for K^+ loss include activation of Gardos channel and KCl transport. These stressors (oxidative stress and K^+ efflux) make erythrocytes defective and in order to escape hemolysis erythrocytes opt for suicidal death [10]. One of the crucial molecules regulating suicidal death of erythrocyte is the death receptor Fas [11]. Fas mediated erythrocyte death has been observed in other metal toxicities [12].

Conventional and alternative medical treatments for chronic Pb^{2+} toxicity includes chelation therapy with meso-2,3-dimercaptosuccinic acid (DMSA) and monoisoamyl DMSA (MiADMSA) [13,14]. However, these chelators are potentially toxic and often fail to remove Pb^{2+} from all body tissues [15]. These chelators are hydrophilic and lipophobic, so they cannot cross the cell membrane to remove intracellular Pb^{2+} [14]. These chelators also do not provide protection in terms of biochemical recovery in the cellular environment [16]. Administration of vitamins C and E supplements augment the function of endogenous free radical scavengers and decrease the deleterious effects of ROS on the cells during Pb^{2+} toxicity. However, studies reveal that when these vitamins are administered in conjunction with a cysteine-based molecule it could ameliorate Pb^{2+} toxicity in a better way than vitamins alone [17].

Garlic (*Allium sativum* Linn.) is well known for its medicinal attributes. Clastogenic effects of the heavy metals are pronouncedly reduced by dietary administration of garlic [18,19]. The potency of garlic in protecting cells from the adverse effect of heavy metals was attributed to the antioxidant activity and chelating efficacy of garlic [20]. Some studies have revealed that garlic was superior to 2,3-dimercapto-1-propanol, D penicillamine, DMSA and N-acetyl-D-penicillamine treatment in metal toxicity [21]. The active ingredients of garlic include lipophilic sulfur-bearing compounds [22,23]. Flavor and aroma molecules of garlic are also due to the presence of organosulfur compounds that are derivatives of the amino acid cysteine [22]. The organosulfur compounds have an antioxidant property and have no known toxicity at a therapeutic dose [23]. The purpose of the present study was to evaluate the role of the two bioactive sulfur compounds SAC and DADS, in potentiating the lifespan of erythrocytes. Our results revealed that sulfur compounds partially prolonged the survival time of erythrocytes. When a sulfur compound from garlic was combined with Gardos channel inhibitor CLT, the lifespan of erythrocytes were completely restored. This study explores the potential benefits of combining organosulfur compounds with Gardos channel inhibitor in accentuating the survival of erythrocytes during Pb^{2+} toxicity.

2. Materials and methods

2.1. Materials

Radioactive sodium chromate (labeled with ^{51}Cr; sp act 94.2 Ci/g) was procured from Board of Radiation and Isotope Technology (Mumbai, India). Nitrocellulose membrane and Amicon Ultra 30 kDa were obtained from Millipore Corporation (Billerica, MA, USA). Amplex® Red Sphingomyelinase Assay Kit, 3′-(phydroxyphenyl) fluorescein (HPF), AP-Rabbit anti-Mouse IgG (secondary) and Alexa Fluor 633 goat anti mouse (secondary) antibodies were procured from Invitrogen Ltd. (Eugene, Oregon, USA). Mouse monoclonal anti-Fas and mouse monoclonal anti-β actin antibodies were bought from Santa Cruz Biotechnology (Santa Cruz, CA, USA). Caspase 3 and caspase 8 assay kits were purchased from Biovision Inc. (Mountain View, CA, USA). SGPT and SGOT measurement kits were obtained from TECO Diagnostics (Anaheim, CA, USA). Glutathione S transferase (GST) was obtained from Cayman chemicals (Ann Arbor, Michigan, USA). All other fine chemicals (unless mentioned) were purchased from Sigma-Aldrich Corporation.

2.2. Animals and treatment

Animal experiments were carried out in female BALB/c mice (12–14 g) bred in-house and maintained with free access of food and water. Ethical guidelines of animal ethics committee of Indian Institute of Chemical Biology, on handling and use of experimental animals were followed during the conduct of the study. Experiments were designed to minimize animal suffering and to use the minimum number associated with valid statistical evaluation. Before commencement of experiments animals of both control and experimental groups were kept separately under standard controlled condition and were fasted for 12 h with free access to water. Lead acetate [$Pb(CH_3COO)_2$], was dissolved in water and administered to animals daily through oral gavage. After the experiments started mice in all groups were provided with fresh food daily. The animals were exposed to (10 mg of Pb^{2+} kg^{-1} body weight) for a period of 15 days. Pb^{2+} exposure was stopped during drug therapy. The drug was diluted appropriately so as to obtain the required dose in 0.05 ml volume, which was administered orally to Pb^{2+} exposed animals (from day 16th of Pb^{2+} exposure) for a period of 10 days. Mineral oil was used as the solvent for DADS preparation. SAC and CLT were dissolved in water. Animals received SAC or DADS orally, daily, in doses ranging from 150 to 250 mg kg^{-1} body weight and CLT at the dose of 25–60 mg kg^{-1} body weights. Drug treated Pb^{2+} exposed mice were grouped according to dose of drug treatment with 6 animals in each group. Control animals received an equivalent amount of distilled water (vehicle) by oral feeding. Mice were euthanized 24 h after receiving the last dose of drug.

2.3. RBC preparation

Whole blood from mice were collected from the retroorbital sinus vein into tubes containing 40 U/ml sodium heparin. WBCs were separated from plasma by centrifugation (180 ×*g*, 20 min, 22 °C), washed 3 times with a saline buffer, and resuspended at a 2% hematocrit according to standard procedure [24].

2.4. Toxicity tests and assessment of metals

Blood was collected in non-heparinized tubes for serum separation. The activity of serum glutamate pyruvate transaminase (SGPT, EC 2.6.1.2), serum oxaloacetate transaminase (SGOT, EC 2.6.1.1), serum urea and serum creatinine were determined colorimetrically according to standard procedures using a commercially available diagnostic laboratory kit. Pb^{2+} content of the whole blood was measured by atomic absorption spectroscopy (Perkin Elmer, AAnalyst 700, Waltham, USA) following the standard protocol [25]. Erythrocyte K^+ concentrations were determined using an atomic absorption spectrophotometer in the emission mode. Measurements were made on erythrocytes after washing for 4 times with isotonic $MgCl_2$ and then lysed in 0.1% LiCl.

2.5. Morphologic characterization of erythrocytes

Packed erythrocytes were fixed in 2% glutaraldehyde dissolved in phosphate buffer saline (PBS) at pH 7.4 in a polyethylene tube. The erythrocytes were gently inverted and allowed to settle for 2 h. Samples were then pipetted to collagen-coated cover slips in a moist petri dish. Cells were then dehydrated through ascending ethanol solutions, processed through critical point, dried in liquid carbon dioxide and coated with gold-palladium. Coated samples were examined in

Jeol Scanning Electron Microscope; model JSM 5200, Tokyo, Japan at 20 kV. 200 to 1200 cells were counted for each sample. Erythrocyte shapes were compared between various groups [24].

2.6. Measurement of lifespan of red cells

Red cell survival was measured from the half-life of erythrocyte over time according to the standard method [26,27]. Briefly, [^{51}Cr]-labeled sodium chromate (specific activity 1.27×103), was injected into mice via the cavernous vein at the dose of 20 μCi/kg. Blood was collected from mice and volumes of erythrocytes were calculated from blood volume. Erythrocytes were washed in 20 mM HEPES–Tris (pH 7.4) and then lysed by adding distilled water. The radioactivity of lysates was measured using a gamma-counter (K2700B/ECIL). Radioactivity present in the red cells was calculated. The count obtained on the first day of injection was taken as 100% value. The radioactivity present in each sample on any subsequent day is related to this initial 100% value as percent of initial activity. The day at which 50% radioactivity disappeared was termed as $t_{1/2}$.

2.7. Flow cytometry

PS exposure was detected by the specific binding of FITC-conjugated annexin V (annexin V-FITC). 10 μl of washed erythrocytes (5×10^6 erythrocytes) were incubated in HEPES buffer with saturating concentrations of fluorescein isothiocyanate (FITC)-conjugated annexin V (4 μg/ml) in the dark for 20 min at room temperature, followed by washing with HEPES buffer. FITC signal was detected using a 488 nm excitation light on a FACS Calibur instrument (BD Bioscience, Mountain View, CA, USA) [28]. For each experiment, fluorescence signals of unstained erythrocytes (autofluorescence) were measured and used to adjust the fluorescence intensity of annexin-V stained erythrocytes. Data were analyzed using Cell Quest software attached with the flow cytometer. Analysis of forward scatter and FL-1 fluorescence was performed without gating. In each sample run, at least 10,000 events were acquired.

2.8. Measurement of $OH^{\bullet-}$ generated within erythrocytes

The intracellular hydroxyl radical ($OH^{\bullet-}$) accumulation was measured using a cell-permeable fluorescent dye HPF [26]. HPF (4 μl, 1 mM) was injected in the tail veins of mice. Blood was collected by intracardiac puncture from ketamine-anesthetized mice. Erythrocytes were isolated and washed twice with HEPES buffer (pH 7.4). HPF fluorescence intensity is parallel to the amount of ROS formed within the cells [29]. The fluorescence of the samples was estimated in a microplate fluorimeter (Perkin Elmer, Model LS55, Llantrisant, UK) at excitation: 485 nm and emission: 520 nm.

2.9. GSH and GSH–HNE adduct measurement

Red cells were washed three times with 0.154 M NaCl. Cell samples were lysed by adding 3 volumes of 5 mM imidazole–HCl at pH 7.0. After the lysate was stirred for 45 min, it was centrifuged for 20 min at 25,000×g. Reduced glutathione (GSH) was measured in the supernatants using DTNB [30]. Mass spectrometry was used to detect GSH–HNE adduct [31]. Erythrocytes were washed in 4 volumes of 50 mM sodium phosphate, pH 7.4, and kept on ice. Proteins were precipitated from erythrocytes by addition of equal volumes of ice-cold ethanol followed by centrifugation for 30 min at 17,000×g with a temperature at 4 °C. The supernatants were collected and stored at −20 °C until further analysis. Mass spectra of the supernatant were taken in the positive-ion mode in Waters Micromass Q-TOF Micro TM mass spectrometer (Milford, MA, USA) using electrospray ionization.

2.10. GST assay

Erythrocytes were lysed with hypotonic PBS (30 mOsm). Cell lysates was centrifuged at 3000 rpm for 15 min at 4 °C. Aliquots of the supernatants were utilized for enzymatic assays. GST was assayed spectrophotometrically using a GST assay kit at 340 nm by measuring the rate of 1-chloro-2,4-dinitrobenzene (CDNB) conjugation with GSH. One unit of GST activity was calculated as nmol CDNB conjugate formed/min, using a molar extinction coefficient of $9.6\times10^3\ M^{-1}\ cm^{-1}$.

2.11. Determination of redox potential of erythrocytes

Redox potential in RBC was determined from the ratios of pyridine nucleotides. Redox potential was assayed from NADH/[NAD^+ + NADH] and NADPH/[$NADP^+$ + NADPH] ratios [24].

2.12. TBARS measurement

Fresh erythrocytes were centrifuged and suspended in PBS. The erythrocyte membrane was prepared by the method of Dodge et al. [32]. Concentration of thiobarbituric acid reactive substance (TBARS) was measured by the spectrophotometric method based on the reaction of lipid peroxides with thiobarbituric acid (TBA). Measurements were done at 532 nm, using malonaldehyde bis (Bimethyl Acetal) as standard [33]. Quantitation was based upon the molar extinction coefficient of $1.56\times105\ M^{-1}\ cm^{-1}$ and the MDA content was expressed in nmol per mg protein.

2.13. Immunoblot analysis

Erythrocyte lysates and membranes were prepared as described above [32]. Erythrocyte membrane suspensions and lysates of erythrocyte ghosts were resolved on 12.5% SDS-PAGE under nonreducing conditions, and then transferred to nitrocellulose membrane. The nitrocellulose membrane was blocked with 5% skimmed milk powder in PBS, probed with anti-Prx2 antibody at an appropriate dilution, washed and then incubated with ALKP-conjugated goat anti-rabbit secondary antibody at an appropriate dilution. The membrane was washed and immunoreactive proteins were finally visualized using color developing reagent BCIP/NBT. The blots were scanned densitometrically to estimate the percentage of degradation of the membrane proteins.

2.14. Determination of caspase activities

Erythrocytes were suspended in 100 ml of lysis buffer (50 mM Tris–Hcl containing protease inhibitor cocktail) and centrifuged at 12,000×g for 10 min at 4 °C. The proteolytic activity of caspase 3 and caspase 8 were evaluated in erythrocyte lysates using the fluorometric substrates DEVD-AFC (caspase-3 substrate) and IETD-AFC (caspase-8 substrate), following the protocols of the Caspase Activity Assay kits. The activity was monitored as the linear cleavage followed by release of the AFC side chain and was compared with a linear standard curve generated on the same microplate.

2.15. Phthalate density profile

Phthalate density profile was used to determine alterations in the cellular density of the entire red cell population. Density distribution curves were obtained using phthalate esters in microhematocrit tubes according to standard procedure [34].

2.16. Determination of Gardos channel activity

Erythrocytes were suspended in the incubation medium (125 mM NaCl, 25 mM $NaHCO_3$, 5 mM KCl, 1 mM $CaCl_2$, 0.15 mM $MgCl_2$, 10 mM

Tris–MOPS, 10 mM glucose and 10 mM sucrose at pH 7.4). ^{86}Rb was added as a radioactive tracer for K^+ ions and aliquots of the suspension were taken at 20, 40, and 60 min after addition of the tracer [35]. ^{86}Rb flux was terminated by immediate dilution of the ^{86}Rb with excessive amounts of ice-cold washing solution containing 100 mM $Mg(NO_3)_2$ and 10 mM imidazole titrated with HNO_3 at pH 7.4 on ice. Cells were washed for 3 times to remove extracellular radioactive ^{86}Rb. Cells were then deproteinized with 0.2 ml of 5% trichloroacetic acid. The amount of ^{86}Rb in the medium and deproteinized cell pellet extracts were measured with a liquid scintillation counter (Wallac 1409, Rockville, USA).

2.17. Activity of cellular antioxidants

Activity gel assays were performed to quantify the activity of catalase and GPx [31]. Catalase activity gels were developed by soaking the non-reducing SDS-PAGE of the enzyme source first in horseradish peroxidase (50 μg/ml) for 45 min in 50 mM phosphate buffer (pH 7.0) followed by addition of 5 mM H_2O_2. The gels were scanned densitometrically to estimate the percentage of membrane proteins degradation. For GPx activity gel assay, total proteins of each sample were separated in a native 12.5% polyacrylamide gel [30]. The gel was first rinsed in distilled water three times and then incubated in 1 mM glutathione and 0.008% cumene hydroperoxide for 10 min. The gel was then stained with 2% ferric chloride and 2% potassium ferricyanide. Achromatic bands appeared on the gel were scanned densitometrically to estimate the percentage of degraded membrane proteins.

2.18. Determination of ceramide

Ceramide contents in erythrocytes were determined by antibody based fluorimetric method [36]. Erythrocytes (2×10^5 cells) were permeabilized with 0.1% Triton X-100 and 0.1% bovine serum albumin for 3 min at room temperature. The permeabilized erythrocytes were then incubated with anticeramide mAb, followed by FITC-labeled secondary antibody and the generation of ceramide was analyzed by Perkin-Elmer spectrofluorimeter (LS55, UK) at excitation: 488 nm; emission: 519 nm in FACS (BD Biosciences, Mountain View, CA, USA).

2.19. Measurement of aSMase activity

To quantify aSMase activity, erythrocytes (5×10^{10} cells) were resuspended in Triton lysis buffer (containing 250 mM sodium acetate 1 mM EDTA and 0.1% Triton-X 100 at pH 5.0). Cellular debris was removed by centrifugation at 3000×*g* at 4 °C and supernatant was collected. 100 mg of protein from the supernatant fraction was used to measure aSMase activity by Amplex® Red Sphingomyelinase Assay Kit using sphingomyelin as the substrate [37]. The fluorescence intensity of the product (excitation: 560 nm; emission: 590 nm) was quantified using Perkin-Elmer spectrofluorimeter (LS55, UK).

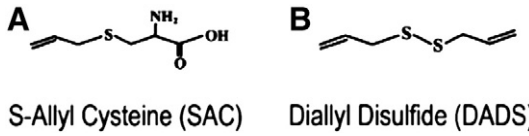

Fig. 1. Chemical structures of (a) S allyl cysteine (SAC) (b) di allyl disulfide (DADS).

2.20. Isolation of lipid rafts

Lipid rafts were isolated from erythrocytes by discontinuous density gradient ultracentrifugation [38]. Erythrocytes were lysed on ice in 800 μl of raft lysis buffer (0.5% Triton X-100, 0.1 M Na_2CO_3, protease inhibitor cocktail, 5 mM iodoacetic acid, 10 μM zVAD, 150 mM NaCl, 15 mM EDTA and 10 mM Tris–HCl). In an ultracentrifuge tube, gradients were prepared by mixing 666 μl of lysate with 1.33 ml of 60% optiprep followed by an overlaying with 7.5 ml of 30% optiprep (diluted with 150 mM NaCl, 15 mM EDTA, 10 mM Tris–HCl, complete protease inhibitor cocktail and 5 mM IAA) followed by 3 ml of 5% optiprep (diluted with 150 mM NaCl, 15 mM EDTA, 10 mM Tris–HCl, protease inhibitor cocktail and 5 mM IAA). Gradients were spun for 9 h at 4 °C at 200,000×*g*. Gradients were then fractionated, mixed with lithium dodecyl sulfate-containing loading buffer and DTT, separated by 12% SDS PAGE and immunoblotted for Fas. Flotillin-2 was used as a marker protein for lipid raft microdomains.

2.21. Fas aggregation on erythrocyte membrane

Thin-smear of 5% erythrocyte in PBS was used for immunohistochemistry with Fas antibody [39]. After fixing in acetone for 10 min at −20 °C, slides were incubated with 1:50 normal horse serum for 30 min at room temperature. Slides were then washed in PBS and incubated with anti-Fas antibody diluted at 1:500 in PBS for 1 h. The slides were then washed twice with PBS and further incubated with Alexa Fluor 488-tagged secondary antibody (1:5000) for 30 min at room temperature. Fas aggregation on the erythrocyte cell surface was studied under confocal microscope (Leica Microsystems, Model GmBH, Heidelberg, Germany).

2.22. Statistical analysis

All data are given as mean ± S.D. Differences between two groups were compared by unpaired Student's *t*-test. For multi group comparisons, analysis of variance was determined by ANOVA followed by Student–Newman–Keuls test. A value of $P<0.05$ was considered statistically significant.

3. Results

3.1. SAC in combination with CLT restores the lifespan of erythrocytes more efficiently than DADS and CLT combination

Allyl sulfur compounds are responsible for the biological and medical functions of garlic [40]. Fig. 1A and B shows the structure of two organosulfur compounds of garlic S allyl cysteine (SAC) and Diallyl

Fig. 2. Attenuation of Pb^{2+} induced decreased survival of erythrocytes in response to SAC, DADS and CLT treatment. Co-relation between decrease in lifespan of erythrocytes and (A) intracellular ROS generation ($OH^{\bullet-}$ content). (B) K^+ efflux (% decrease in K^+ content) at different periods of Pb^{2+} exposure. $OH^{\bullet-}$ content was determined spectrofluorometrically using HPF as fluorescent probe. K^+ content was determined using atomic absorption spectrometer as described under Materials and methods section. Values are representative of three independent experiments (n = 6). (C–I). Survival of erythrocytes was studied using radiolabeled Cr^{51}. Cell associated radioactive count within 24 h of Cr^{51} was designated as 100%. Cell survival was determined from the day showing 50% decay of radioactivity (represented as $t_{1/2}$ in day). Drug treatment started after 15 days of Pb^{2+} exposure. Details of treatment schedule are given under Materials and methods section. Survival of erythrocytes treated with (C) SAC (150–250 mg/kg body weight/day) for 7 days (D) SAC 200 mg/kg body weight g/day) for up to 20 days (E) DADS (150–250 mg/kg body weight/day) for 7 days (F) DADS (200 mg/kg body weight/day) for 5 to 20 days (E) CLT (25–60 mg/kg body weight/day) for 7 days and (H) CLT (50 mg/kg/day) for up to 20 days. Radioactive count in the red cells was taken at 4 days interval up to 20 days. $t_{1/2}$ is represented in parenthesis. Values are mean ± SD of three independent experiments (n = 6). (I and J) Decay of Cr^{51} radioactivity in erythrocytes and mean half-life of erythrocytes respectively. Animals were treated with SAC and DADS both at the dose of 200 mg/kg body weight/day, CLT at 50 mg/kg body weight/day, DMSA 50 mg/kg body weight/day for 10 days. Results are mean ± SD of three independent experiments, (n = 6). $^{\#}p<0.01$ vs. respective age matched controls. NS = non significant, $^{*}p<0.05$, $^{**}p<0.01$ vs. respective exposed levels.

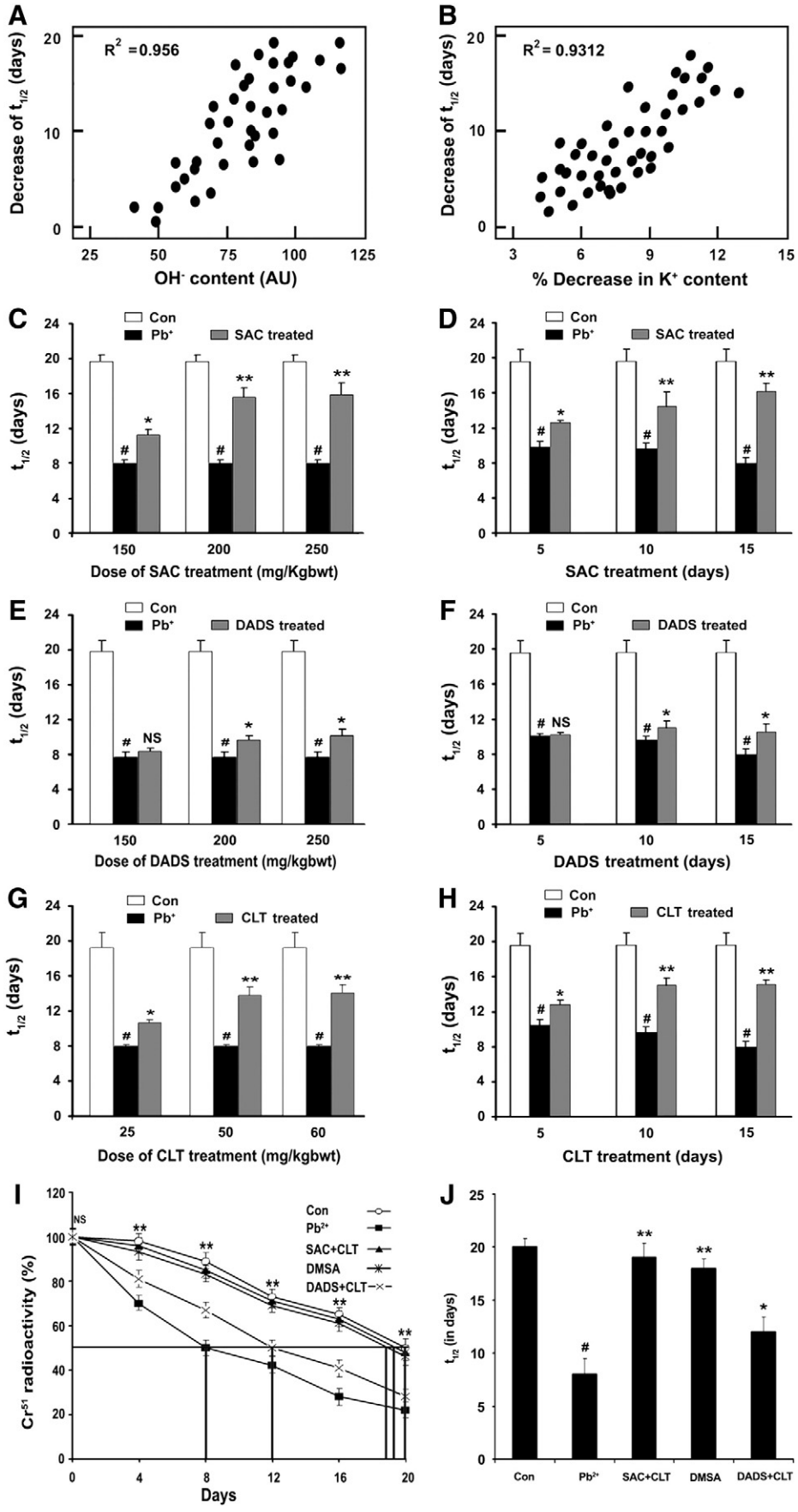
A
R² =0.956
Decrease of t1/2 (days)
OH⁻ content (AU)
B
R² = 0.9312
Decrease of t1/2 (days)
% Decrease in K⁺ content
C
Con
Pb⁺
SAC treated
t1/2 (days)
Dose of SAC treatment (mg/Kgbwt)
D
Con
Pb⁺
SAC treated
t1/2 (days)
SAC treatment (days)
E
Con
Pb⁺
DADS treated
NS
t1/2 (days)
Dose of DADS treatment (mg/kgbwt)
F
Con
Pb⁺
DADS treated
NS
t1/2 (days)
DADS treatment (days)
G
Con
Pb⁺
CLT treated
t1/2 (days)
Dose of CLT treatment (mg/kgbwt)
H
Con
Pb⁺
CLT treated
t1/2 (days)
CLT treatment (days)
I
Con
Pb²⁺
SAC+CLT
DMSA
DADS+CLT
NS
Cr51 radioactivity (%)
Days
J
t1/2 (in days)
Con
Pb²⁺
SAC+CLT
DMSA
DADS+CLT

disulfide (DADS or 4,5-dithia-1,7-octadiene). These two organosulfur compounds have thioallyl skeletal structure. SAC exhibited substitution on the S-allyl skeleton with the alanyl group (Fig. 1). Our results indicated that a positive correlation exists between $OH\bullet^{-}$ generation and reduction in lifespan of erythrocytes in mice during Pb^{2+} exposure (Fig. 2A). Loss of K^{+} from erythrocytes was also positively correlated with the reduction in lifespan of erythrocytes (Fig. 2B). The results indicated that $OH\bullet^{-}$ generation and K^{+} loss in erythrocytes might be involved in the shortening of their lifespan. These results form a strong rationale for evaluation of compounds with an antioxidant property and inhibitor of the K^{+} channels, for preventing the decline in the lifespan of erythrocytes in mice exposed to Pb^{2+}. Biologically active compounds of garlic with a known antioxidant property included in our study were SAC and DADS. Fig. 2C revealed that SAC treatment enhanced the lifespan of erythrocytes progressively with an increase in the dose. The lifespan of erythrocytes increased during SAC treatment, which reached threshold level at 200 mg kg^{-1} body weight but a further increase in SAC concentration failed to furnish better results. Thus we selected a 200 mg kg^{-1} body weight dose of SAC for the subsequent experiments. The studies on the optimum time period of SAC treatment revealed that the lifespan of erythrocytes in Pb^{2+} exposed mice increased to a considerable level within 10 days of treatment after which it did not show further improvement (Fig. 2D). We conducted dose dependent and time period dependent studies with DADS (Fig. 2E and F). However, treatment of Pb^{2+} exposed animals with DADS could partially improve the lifespan of erythrocytes even at the dose of 250 mg kg^{-1} body weight for a treatment period of 15 days. Time dependent and dose dependent studies with CLT, an agent blunting K^{+} loss from cells were undertaken. CLT could partially restore the lifespan of erythrocytes in Pb^{2+} exposed mice at a dose of 50 mg kg^{-1} body weight for a period of 15 days (Fig. 2G and H). As monotherapy with either of the active compounds of garlic or Gardos channel inhibitor fell short of the goal of completely restoring the lifespan of erythrocytes in Pb^{2+} exposed mice. As with monotherapy the Pb^{2+} exposed mice failed to achieve desired results we went ahead with the strategy of combining these compounds. DMSA treated Pb^{2+} exposed mice were used as a positive control since DMSA is a standard drug in the treatment against Pb^{2+} exposure. The combination therapy with SAC and CLT was very efficient in restoring the lifespan of erythrocytes, which was better than DADS in combination with CLT and also DMSA treated Pb^{2+} exposed animals (Fig. 2I and J).

3.2. Combination of SAC and CLT is better than DADS + CLT combination in protecting erythrocytes against morphological alterations

Scanning electron micrographs of erythrocytes revealed morphological alterations in the Pb^{2+} exposed mice (Fig. 3A). Most of the cells showed a deeply crenated shape (echinocyte) with some cells having a greater number of spicules than others. Echinocyte formation indicated that erythrocytes had an increased plasma membrane surface area relative to cellular volume. DMSA treatment partially restored the morphological alterations in erythrocytes (Fig. 3B). Monotherapy with SAC and DADS were partially successful in restoring the morphological changes in erythrocytes but SAC monotherapy exerted better effect than DADS monotherapy. During CLT monotherapy cells had blunted spicules with the number of echinocytes declining (data not shown). SAC monotherapy was better than all other monotherapies in restoration of erythrocyte morphology to discocyte. Erythrocytes from animals treated with combination of SAC and CLT significantly attained more normal biconcave disc configurations (discocytes) than those treated with DADS and CLT combination therapy.

3.3. In vitro study: SAC is more potent than DADS in preventing erythrocyte death

To mimic the primary aspects of the response generated in erythrocytes in Pb^{2+} exposed mice we incubated the erythrocytes with Pb^{2+}. The reasons why SAC was better than DADS in providing protection to erythrocyte during Pb^{2+} exposure were evaluated. Erythrocyte deaths were assessed by analyzing forward scatter and annexin V binding studies. The data suggested that decrease of erythrocyte forward scatter by the Pb^{2+} exposed group was inhibited by SAC and DADS. SAC was better than DADS in inhibiting a decrease in cell volume as indicated by forward scatter. CLT also prevented Pb^{2+} induced cell shrinkage. The maximum decrease in cell shrinkage was observed when SAC was combined with CLT (Fig. 4A). The effect of SAC and CLT in combination on forward scatter was paralleled by a significant decrease of annexin V binding in Pb^{2+} exposed erythrocytes (Fig. 4B). SAC offered better protection than DADS against PS exposure in erythrocytes exposed to Pb^{2+}. CLT offered partial protection against PS externalization during Pb^{2+} exposure and it synergistically resisted PS exposure when combined with organosulfur compounds. These results indicate why DADS and CLT combination

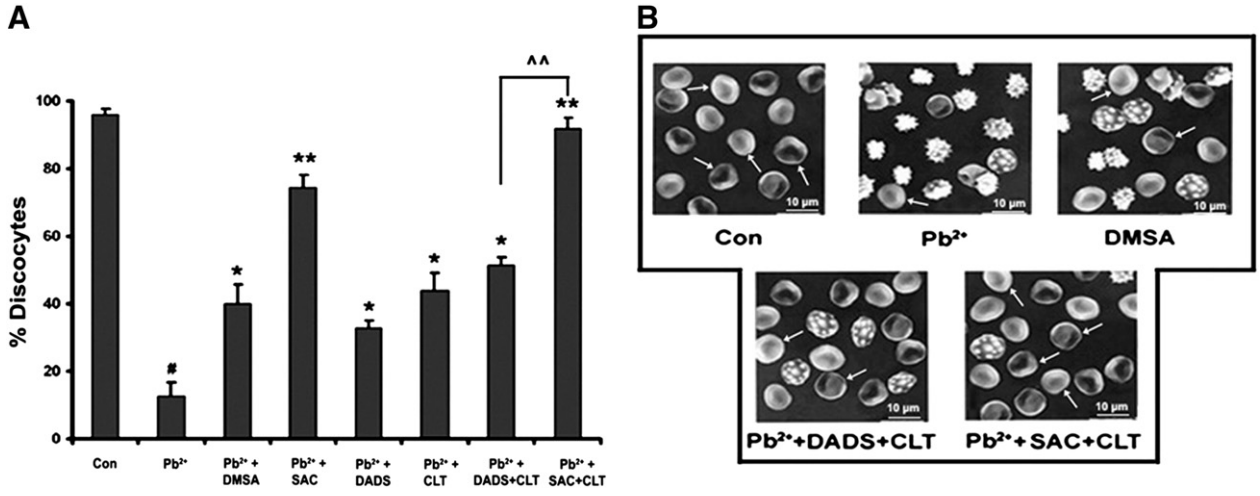

Fig. 3. Pb^{2+} induced morphologic alteration of erythrocytes before and after drug treatment. Animals were exposed to Pb^{2+} (10 mg/kg body weight/day) for 15 days followed by treatment with either/both SAC and DADS (200 mg/kg body weight/day), CLT (50 mg/kg body weight/day) and DMSA (50 mg/kg body weight/day) for 10 days. % of discocytes was calculated from distribution of erythrocytes as observed under scanning electron microscope (A). (B) SEM images of discocyte (indicated with arrows). Samples were prepared for SEM analysis as described under Materials and methods section. Results are representative of three independent experiments. Values are mean ± SD of three independent experiments, (n = 6). $^{\#}p<0.01$ vs. respective age matched controls. NS = non significant, $^{*}p<0.05$, $^{**}p<0.01$ Pb^{2+} exposed groups.

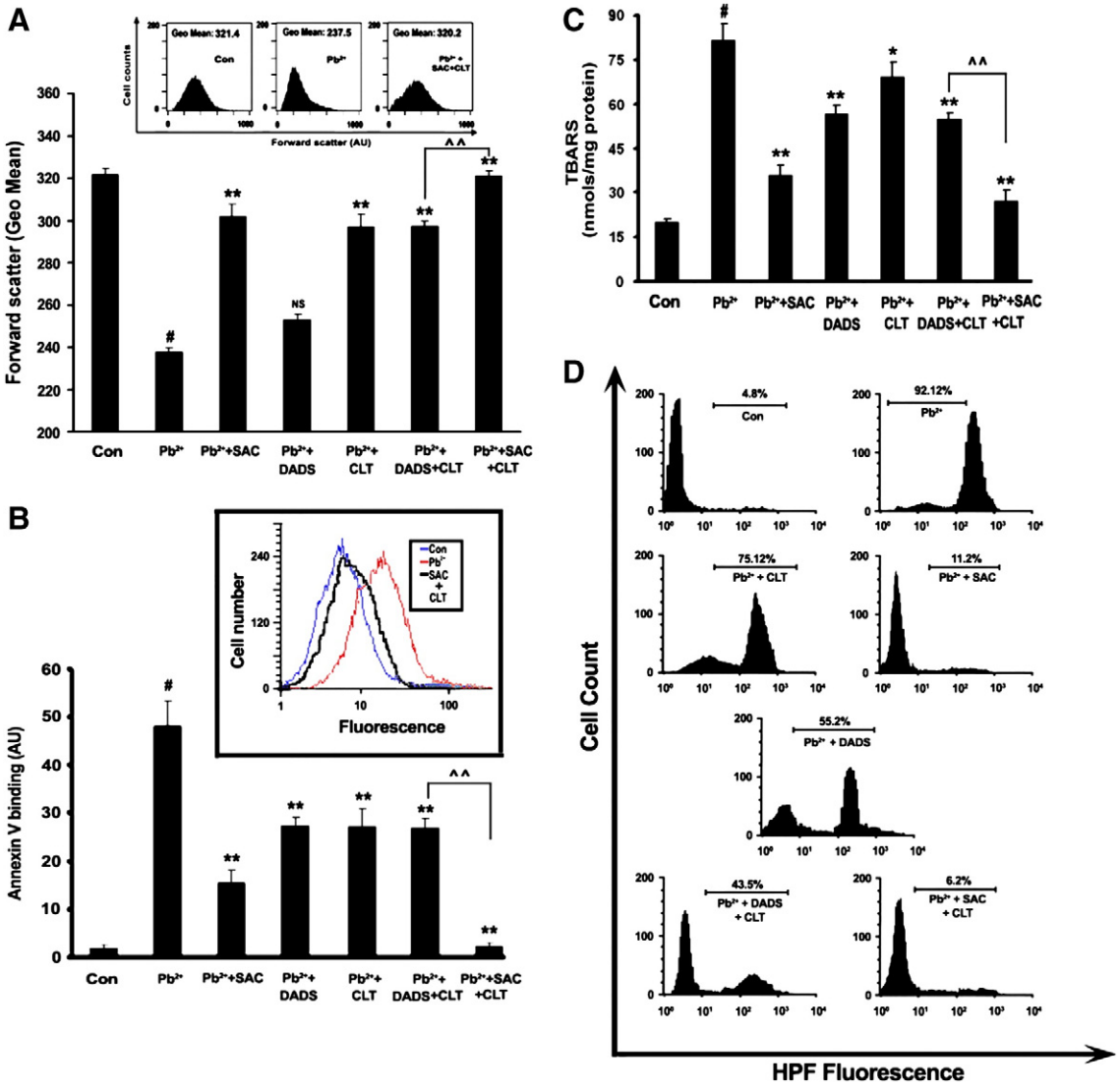

Fig. 4. *In vitro* studies: treatment with SAC, DADS and CLT controls decreased forward scatter, increased PS exposure and increased ROS generation in Pb^{2+} exposed red cells. 5×10^5 erythrocytes were incubated with lead acetate [$Pb(CH_3COO)_2$,1 mM] for 9 h at 37 °C. Cells receiving drug treatment were preincubated with different drugs for 30 min before exposure with Pb^{2+}. Drugs used are 0.5 mM SAC, 0.5 mM DADS and 0.1 μM CLT. Cells receiving combination treatment were incubated with 0.1 μM CLT and 0.5 mM SAC and 0.1 μM CLT and 0.5 mM DADS. Cells receiving no treatment served as control group. (A) Forward scatter of erythrocytes was measured flow cytometrically and expressed as geo means in the respective cell population. Inset: histogram showing decreased forward scatter in Pb^{2+} exposed cells with combination of SAC and CLT. Results are representative of three independent experiments with similar results (n = 6). Values are mean ± SD, #p<0.01 vs. control cells. NS = non significant, **p<0.01 vs. Pb^{2+} exposed groups. ^^p<0.05 vs. Pb^{2+} exposed cells with DADS + CLT treatment. (B) Externalization of PS represented as percentage of annexin-V positive cells in the respective cell population. Inset: histogram of annexin-V binding in red cells. Control (blue scan), Pb^{2+} exposed (red scan) and Pb^{2+} + SAC + CLT (black scan). Results are representative of three different experiments (n = 6). Values are mean ± SD, #p<0.01 vs. control cells. **p<0.01 Pb^{2+} exposed cells. ^^p<0.05 vs Pb^{2+} exposed cells with DADS + CLT treatment. (C) Effect of monotherapy and combination therapy with SAC, DADS, and CLT on lipid peroxidation in Pb^{2+} red cells. Values are mean ± SD of three separate experiments (N = 6), #p<0.01 vs. control cells. *p<0.05 and **p<0.01 Pb^{2+} exposed cells. ^^p<0.05 vs. Pb^{2+} exposed cells with DADS + CLT treatment. (D) Presence of $OH^{\bullet-}$ was determined flow cytometrically from the histograms showing oxidation of HPF. Results are representative of three independent experiments.

exerted inferior protection to erythrocytes than SAC and CLT combination in the restoration of its lifespan during Pb^{2+} exposure.

Oxidative stress is one of the most common events that trigger the apoptosis of red cells. Based on this we evaluated TBARS in the erythrocyte membrane exposed to Pb^{2+}. Pb^{2+} induced an increase in TBARS, which could be inhibited when the cells were preincubated with SAC and DADS. SAC offered better protection against oxidative stress than DADS and this explains the capability of SAC in offering better protection to PS exposure in Pb^{2+} exposed erythrocytes. CLT also exerted antioxidant effect and could prevent formation of TBARS, although to a lesser extent than SAC or DADS. When SAC or DADS was preincubated in combination with CLT, they could exert

Table 1
Total Pb^{2+} content in whole blood.

Groups	Con	Pb^{2+}	Pb^{2+} + SAC	Pb^{2+} + CLT	Pb^{2+} + SAC + CLT
Pb^{2+} content(μg/dl)	2.12 ± 0.03	110.07 ± 20.18[a]	10.83 ± 2.16[**]	98.29 ± 18.39[NS]	7.01 ± 1.65[**]

All data are expressed as mean ± SD. Data are representative of six separate experiments with 6 animals in each group. Unpaired *t*-test was applied to determine the statistical significances.
NS = nonsignificantly different from Pb^{2+} exposed.
[a] Significantly different from control at p<0.001.
** Significantly different from Pb^{2+} exposed at p<0.001.

better influence in combating oxidative stress than single agent alone. SAC and CLT acted synergistically in preventing the formation of TBARS (Fig. 4C) and were better than DADS and CLT. ROS are common mediators for apoptosis, and Pb^{2+} exposure to erythrocytes increased generation of $OH\bullet^{-}$ radicals to a greater extent (Fig. 4D). SAC pretreatment could neutralize $OH\bullet^{-}$ radicals in a better way than DADS. This explained why SAC was better than DADS in inhibiting oxidative stress in Pb^{2+} exposed erythrocytes. Although CLT alone did not offer much protection against generated $OH\bullet^{-}$ radicals, but when combined with SAC it exerted a synergistic effect and rescued the cells from Pb^{2+} induced generation of $OH\bullet^{-}$. SAC and CLT in combination were better than DADS and CLT combination in protecting cells against generation of $OH\bullet^{-}$.

3.4. Combination of SAC and CLT prevents erythrocyte death under in vivo conditions

As the combination of SAC and CLT showed better advantage over DADS and CLT combination in rescuing the erythrocytes during Pb^{2+} exposure, we used SAC and CLT combination for our further study. Table 1 demonstrated that monotherapy with SAC led to a significant removal of Pb^{2+} from blood. Although CLT monotherapy was not efficient as SAC monotherapy in decreasing Pb^{2+}, the success of combination therapy could be attributed to the presence of SAC in combination with drugs. We further evaluated if the combination of SAC and CLT induced any toxicity in mice. Combination therapy had no renal or hepatic toxic effect on mice with or without exposure to Pb^{2+} (Table 2).

We explored the possible mechanisms of the protection offered by SAC and CLT during combination therapy in Pb^{2+} exposed mice. Similar results were observed under both *in vitro* and *in vivo* studies. Cell membranes of erythrocytes in Pb^{2+} exposed mice containing a higher proportion of PS in the outer bilayer with a parallel decrease in forward scatter (Fig. 5A and B). In agreement with our *in vitro* results, erythrocytes from Pb^{2+} exposed mice treated with SAC and CLT displayed less externalized PS molecules than those undergoing monotherapy with either of the agents. SAC and CLT in combination could restore another hallmark of apoptotic cell death, i.e. cell shrinkage, in a better way than monotherapy with either of these agents. SAC monotherapy exhibited a slight advantage over CLT monotherapy with regard to restoration of forward scatter in Pb^{2+} exposed mice. Density distributions of erythrocytes were determined using the phthalate method. The phthalate density distribution of erythrocytes from Pb^{2+} exposed mice undergoing combination therapy were shifted toward lower densities, suggesting that the steady state volume homeostasis of the cells were restored to normal level (Fig. 5C). Similar to forward scatter results SAC showed a slight advantage over CLT when administered as monotherapy but showed a synergistic effect when administered in combination.

Table 2
Erythrocyte intracellular serum glutamate pyruvate transaminase (SGPT), serum oxaloacetate transaminase (SGOT), serum urea and serum creatinine content.

Parameter	Con	Con + SAC + CLT	Pb^{2+}	Pb^{2+} + SAC + CLT
SGPT (IU/l)	19.16 ± 3.25	17.0 ± 3.00^{NS}	510.0 ± 14.26[a]	27.0 ± 5.12[**]
SGOT (IU/l)	20.7 ± 3.21	17.5 ± 4.00^{NS}	160.0 ± 22.82[a]	25.2 ± 5.05[**]
Serum urea (mmol/l)	27.9 ± 3.32	23.0 ± 4.22^{NS}	105.0 ± 9.13[a]	28.0 + 6.81[**]
Serum creatinine (mg/dl)	1.07 ± 0.06	1.00 + 0.09^{NS}	3.6 ± 1.28[a]	1.33 ± 0.22[**]

All data are expressed as mean ± SD. Data are representative of 6 independent experiments with 6 animals in each group. Unpaired *t*-test was applied to determine the statistical significance.
NS = nonsignificantly different from control.
[a] Significantly different from control at $p<0.001$.
[**] Significantly different from Pb^{2+}. Exposed at $p<0.001$.

3.5. Combination of SAC and CLT restores redox balance in erythrocytes

The redox balance of a cell is an important regulator of apoptosis and so we explored the effect of a SAC and CLT combination on redox balance of erythrocytes, which was downregulated during Pb^{2+} exposure. Although SAC monotherapy reversed the redox potential of the cells to a large extent it was interesting to note that CLT monotherapy had the capability to restore the redox balance of the cell to some extent. The combination therapy efficiently restored the redox potential of cells to a normal level and this could be due to the synergistic behavior of SAC and CLT (Fig. 6A). GSH the most abundant and important intracellular antioxidant in erythrocytes declined in Pb^{2+} exposed mice (Fig. 6B) which was efficiently restored by SAC and to some extent by CLT. The restoration of GSH during combination treatment could be attributed to the presence of SAC treatment mainly.

To analyze the causes that led to the decline of GSH in erythrocytes we assessed the activity enzyme GST that protects cells against toxicants by conjugating the thiol group of the glutathione to electrophilic xenobiotics. In mice exposed to Pb^{2+} GST activity increased significantly (Fig. 6C). CLT monotherapy failed to influence GST activity. However SAC monotherapy and combination of SAC and CLT treatment led to a decrease in GST activity. Under this circumstance GSH is likely to be a major cytosolic target for break down products of lipid peroxidation. Formation of the bifunctional electrophile-GSH adduct (446 and 464 m/z) were observed in erythrocytes of Pb^{2+} exposed mice and these adducts could account for a decrease in cellular GSH. Formation of GSH–HNE adducts were downregulated during SAC monotherapy and combination therapy with SAC and CLT. CLT monotherapy did not influence increased GSH adduct formation during Pb^{2+} exposure (Fig. 6D–G).

3.6. SAC and CLT in combination rehabilitates cellular antioxidant defense

We assessed a set of antioxidant molecules in the erythrocytes of Pb^{2+} exposed mice. We found a significant decrease in antioxidant parameters tested, which included catalase (Fig. 7A), GPx (Fig. 7B), and reduced Prx2 (Fig. 7C). In agreement with this observation there was increase in Prx2 (oxidized) in the cytosol of erythrocytes of Pb^{2+} exposed mice. Monotherapy with SAC resulted in better restoration of antioxidant enzymes (Catalase and GPx and reduced Prx2) than CLT indicating that SAC had more capability than CLT to rescue erythrocytes from ROS during Pb^{2+} toxicity. However combination therapy could restore the antioxidant enzymes to a normal level completely and this could be attributed to the presence of SAC in a combination of drugs. SAC and CLT when administered simultaneously could restore Prx2 in reduced form with concomitant decline in oxidized form in Pb^{2+} exposed animals.

3.7. Impact of combination therapy on Prx2 translocation to membrane

We wanted to explore the association of Prx2 with erythrocyte membrane during Pb^{2+} toxicity. Fig. 8A revealed Prx2 erythrocyte membrane association increased during chronic Pb^{2+} exposure. Membrane translocation of Prx2 declined significantly with SAC monotherapy and combination of SAC and CLT therapy. CLT monotherapy could not decrease much the binding of Prx2 on membrane. It is well known that Prx2 regulates ion transport by associating with the membrane so we assessed the rate of $^{86}Rb^{2+}$ efflux to understand its impact on Gardos channel. Chronic Pb^{2+} exposure to mice enhanced Gardos channel activity in erythrocytes as evident by $^{86}Rb^{2+}$ efflux and less cellular retention of $^{86}Rb^{2+}$ by the erythrocytes (Fig. 8B). CLT is a known inhibitor of Gardos channel and could prevent activation of Gardos channel in animals exposed to Pb^{2+}. The combination of SAC and CLT also had similar effect and this could be

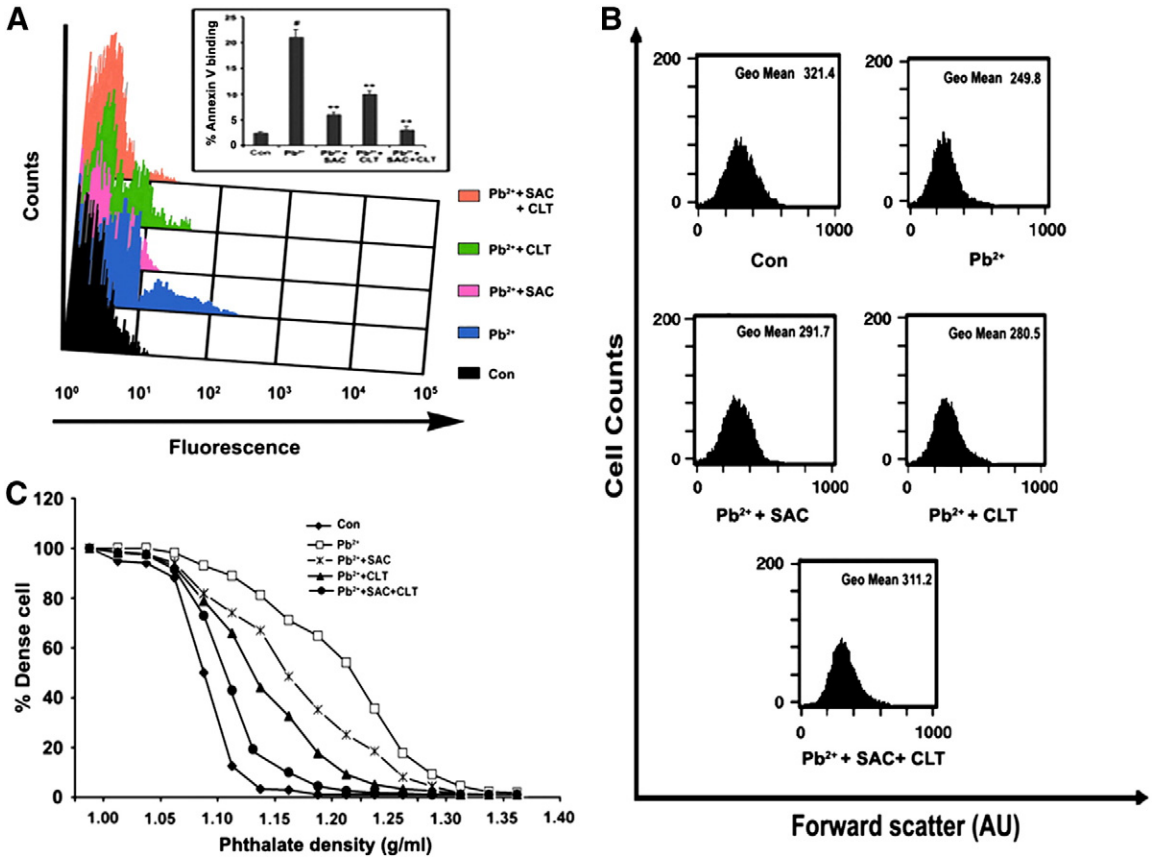

Fig. 5. SAC and CLT treatment restored PS exposure and cell shrinkage in the red cells of Pb^{2+} exposed animals. (A) FACS histograms of annexin-V binding to erythrocyte membrane. Results are representative of three separate experiments. Annexin-V binding was quantified and showing in the inset as % of annexin-V positive cells in the respective cell population. Values are mean ± SD (n = 6), $^{\#}p<0.01$ vs. age matched control cells. $^{**}p<0.01$ Pb^{2+} exposed groups. (B) Forward scatter analysis indicating cell shrinkage. Extent of shrinkage is expressed as geo mean values obtained from the FACS histograms of respective cell population. Results are representative of three separate experiments with similar results (n = 6). (C) Assessment of cell shrinkage from the density distribution of erythrocytes. Density profile of erythrocytes was measured using phthalate gradient density method as described under Materials and methods. Values are mean ± SD of three independent observations with similar results (n = 6).

attributed to the presence of CLT in combination. However it was interesting to note that Gardos channel was partially inhibited by SAC monotherapy. Another consecutive event in erythrocytes of Pb^{2+} exposed mice was aSMase activation (Fig. 8C). Activation of aSMase and ceramide generation in the membrane of erythrocytes of mice undergoing Pb^{2+} exposure could be downregulated by SAC and CLT monotherapies with CLT showing a better advantage than SAC. Combination therapy downregulated aSMase activity in erythrocytes of Pb^{2+} exposed mice. Ceramides are generated from sphingomyelin through activation of aSMases. Abundant ceramides were found in erythrocytes isolated from Pb^{2+} exposed mice, which partially declined during monotherapies and decreased completely during combination therapy with SAC and CLT (Fig. 8D and inset).

3.8. Combination of SAC + CLT prevents Fas aggregation in Pb^{2+} exposed erythrocytes

We found that ceramide generation in erythrocytes during Pb^{2+} exposure were positively correlated with activation of caspase 8, indicating that signal cascades of apoptosis included the generation of a lipid messenger ceramide and activation of caspase cascade (Fig. 9A). The effect of chronic Pb^{2+} toxicity on erythrocyte caspase activity was evaluated using specific fluorometric assays for caspase 3 and caspase 8 (Fig. 9B). Caspase 8 is a membrane-bound mediator initiating the cellular cascade for apoptosis. Caspase 3 is the effector mediator leading to proteolysis of cellular proteins, which get activated in erythrocytes during Pb^{2+} exposure. The activation of caspases (caspase 8 and caspase 3) in Pb^{2+} exposed erythrocytes could be downregulated partially with monotherapies with neither of the agents showing advantage over the other. Combination treatment restrained activation of caspase cascade in erythrocytes during Pb^{2+} toxicity. We wanted to evaluate the upstream events of apoptosis to understand its relationship with ceramide generation. We prepared lipid rafts and studied the translocation of Fas into lipid rafts by immunoblotting the lipid rafts with CD95 antibody. Fig. 9C revealed that Fas was translocated to the lipid rafts during Pb^{2+} exposure. Translocation of Fas to the lipid rafts did not occur in erythrocytes of SAC and combination treated animals. However contrary to the results showing downregulation of caspase 8 during CLT treatment, we found that Fas translocated to lipid rafts of erythrocytes in CLT treated mice. We further evaluated whether the Fas engagement into the lipid raft led to Fas clustering by using confocal microscopy. Our studies demonstrated that the number of cells showing Fas aggregation and cap like appearance of Fas increased in mice exposed to Pb^{2+}. The capped cells declined in the SAC, CLT and SAC + CLT treated Pb^{2+} exposed animals. Although in erythrocytes of CLT treated group Fas was translocated to lipid rafts but it failed to aggregate and take capped appearance (Fig. 9D). These results explain why CLT monotherapy was successful like SAC in attenuating activation of caspase cascade.

3.9. Role of SAC and CLT in translocation of Fas into lipid rafts and in capping of aggregated Fas: in vitro studies

To confirm our results of *in vivo* studies we further conducted *in vitro* studies. Results revealed that Pb^{2+} induced translocation of

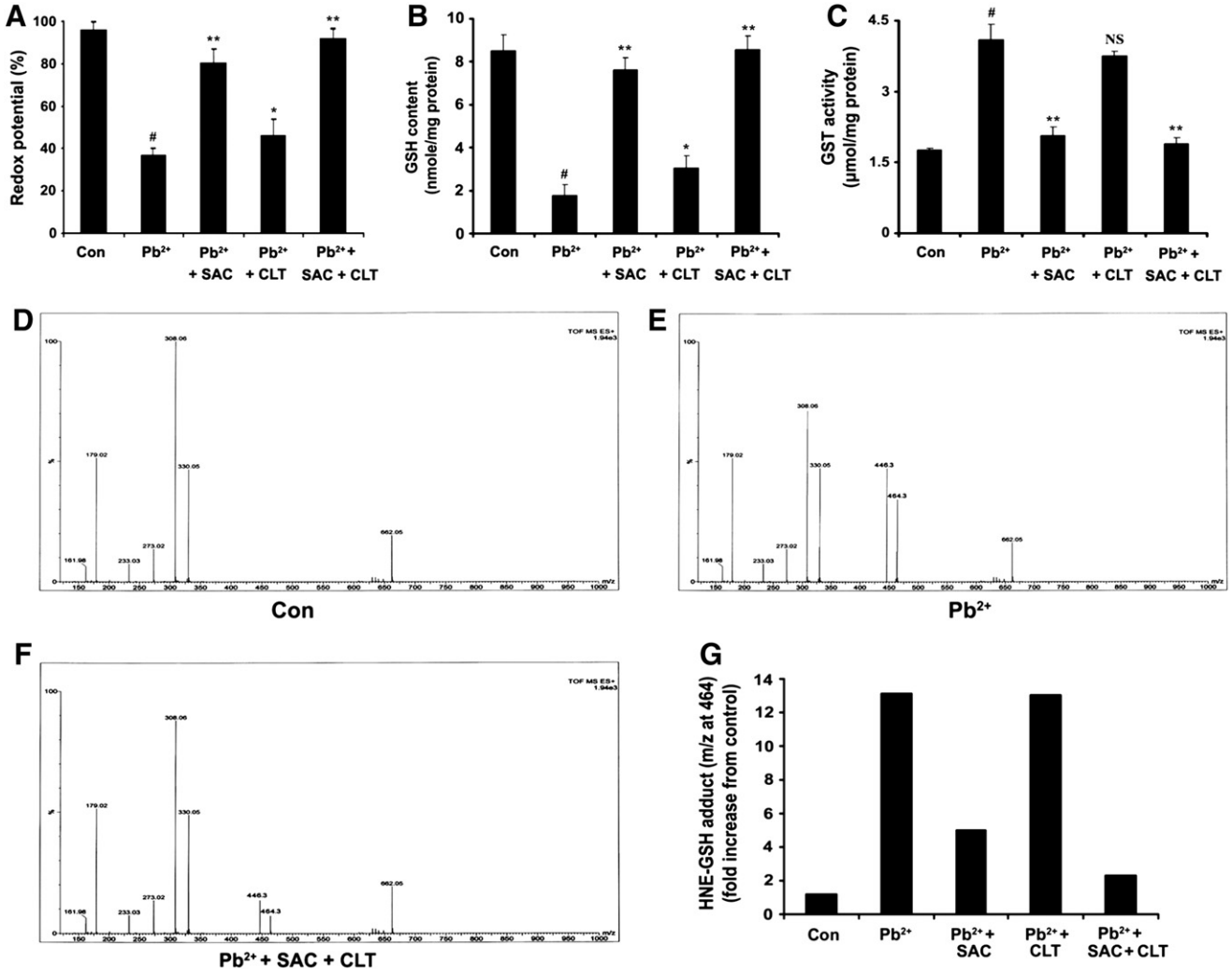

Fig. 6. SAC + CLT treatment down-regulates Pb^{2+} induced decreased redox potential and HNE–GSH adducts formation in erythrocytes. (A) Redox potential in erythrocytes was determined from one ratio of pyridine nucleotide as described under Materials and methods. Results are mentioned mean ± SD of three independent experiments (n = 6), #p<0.01 vs. age matched controls, *p<0.05 **p<0.01 vs. Pb^{2+} exposed. (B) Repletion of Pb^{2+} induced GSH depletion in response to SAC + CLT treatment. Values are mean ± SD of three separate observations (n = 6), #p<0.01 vs. age matched control, **p<0.01 vs. Pb^{2+} exposed. (C) SAC + CLT treatment inactivates GST in erythrocytes of Pb^{2+} exposed animals. Results are mean ± SD of three independent observations (n = 6), #p<0.01 vs. age matched control, NS = non significant and **p<0.01 vs. Pb^{2+} exposed. (D) Mass spectrometer analysis showing the presence of GSH (m/z at 308) in control erythrocytes. Samples were prepared for mass spectroscopy as described under Materials and methods. (E) Mass spectrum showing the major fragment of HNE–GSH adduct formation (m/z at 446 and 464) after Pb^{2+} exposure. (F) Mass spectrum showing restoration of GSH in erythrocytes of Pb^{2+} exposed group after SAC + CLT treatment. (G) Quantitation of HNE–GSH adduct (m/z 464) in erythrocyte lysate of Pb^{2+} exposed animals before and after SAC + CLT treatment. Data shown are representative of 3 experiments with 6 animals in each group.

Fas into lipid rafts in erythrocytes after 9 h of incubation. This could be inhibited by ROS scavenger dimethyl thiourea (DMTU). Imipramine, the aSMase inhibitor failed to rescue the Fas from translocation into lipid rafts. CLT also did not prevent the translocation of Fas into lipid rafts during Pb^{2+} exposure. The $OH^{\bullet -}$ scavenger DMTU prevented translocation of Fas into lipid rafts indicating that ROS generation played a major role in this process. SAC and combination of SAC and CLT prevented translocation of Fas into the lipid rafts, suggesting that SAC during combination therapy might have played a major role in preventing the translocation of Fas into the lipid rafts in the cell membrane (Fig. 10A). We also analyzed the process of aggregation of Fas in the cells exposed to Pb^{2+} using confocal microscopy. Our results revealed that Pb^{2+} exposure to erythrocytes resulted in an increase in the number of cells showing a capped appearance when treated with CD95 antibody, which could be prevented by imipramine pretreatment. The result indicated that activation of aSMase and ceramide generation in the membrane played a vital role in the aggregation of Fas in erythrocytes. Similarly CLT treatment to Pb^{2+} exposed cells decreased the number of cells showing a cap like structure thereby giving credence to our *in vivo* findings and explains why CLT pretreatment downregulated the caspase mediated apoptotic events. The combination of SAC and CLT completely prevented Fas aggregation (Fig. 10B). Imipramine and CLT pretreatment led to a decline in the activity of caspase 8 indicating that activation of Gardos channel leads to cell shrinkage and ceramide generation, which activates the downstream events of Fas mediated apoptosis. SAC and DMTU pretreatment prevented activation of caspase 8 indicating the role of ROS in Fas mediated apoptosis of erythrocytes. Combination of SAC and CLT targeted both the events i.e. ROS generation and Gardos channel and thereby decreasing the apoptotic events in erythrocytes.

4. Discussion

The pathogenesis of Pb^{2+} toxicity is multifactorial, as Pb^{2+} promotes $OH^{\bullet -}$ generation and dehydration of erythrocytes [2,6–8]. The $OH^{\bullet -}$ generated in erythrocytes was positively correlated with decrease in lifespan of erythrocytes, suggesting that $OH^{\bullet -}$ might

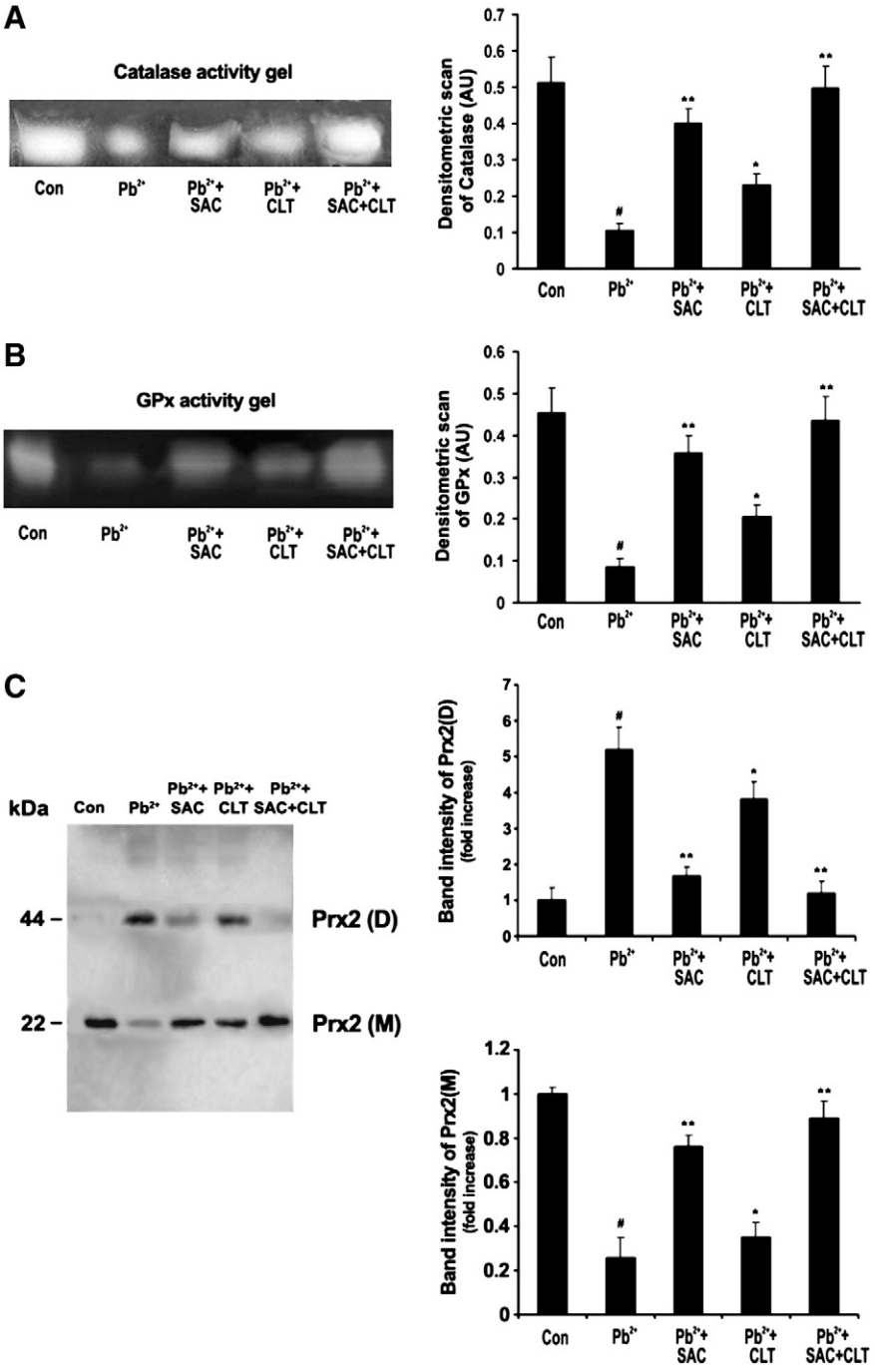

Fig. 7. Regulation of redox status in erythrocytes of Pb^{2+} exposed animals in response to SAC + CLT treatment. SAC + CLT mediated upregulation of Pb^{2+} induced decreased activities of erythrocyte antioxidant enzymes and was detected from representative zymograms (left panels) of (A) catalase and (B) GPx. Densitometric analysis of activity gels are represented in the right panel of (A) and (B). Results are representative of three separate experiments (n = 6), $^{\#}p<0.01$ vs. respective age matched control, $^{*}p<0.05$, $^{**}p<0.01$ vs. respective Pb^{2+} exposed groups. (C) Western blot analysis of SAC + CLT mediated transformation of dimeric Prx2 to monomeric Prx2 in the cytosolic extract from erythrocytes from Pb^{2+} exposed animals. Results are representative of three independent experiments.

have contributed to the accelerated decrease in the lifespan of these cells during chronic Pb^{2+} exposure. The increase in $OH^{\bullet-}$ radical was paralleled by K^{+} loss from the cells. The consequence of loss of K^{+} from the cell is associated with the volume regulatory phase of the cell that culminates in cell shrinkage [9]. Conformational changes in the membrane proteins of the erythrocytes during Pb^{2+} toxicity have been thought to be associated with ion loss in erythrocytes [41,42]. Some reports suggest that Pb^{2+} induced cell shrinkage can be blunted by CLT, an inhibitor of the Gardos channel [43]. Against this background we explored the therapeutic strategies targeting the underlying defects (i.e. oxidative stress and cell dehydration) of erythrocytes during chronic Pb^{2+} toxicity. During the past years, there has been a growing awareness of the potential medicinal uses of garlic [22,23] and various studies indicate that garlic is as effective as conventional antidotes against cadmium and mercury poisoning [44]. The protective effect of garlic extract on metal toxicity is associated, at least in part, to its metal chelating ability [44]. Studies reveal that raw garlic has a protective effect against Pb^{2+} toxicity [45,46]. One of the most interesting of the recent findings is that garlic increases the overall antioxidant levels of the body [23]. The antioxidant properties of garlic, has been mostly ascribed to its high content of sulfur compounds [22,23]. The thiosulfinates of garlic are

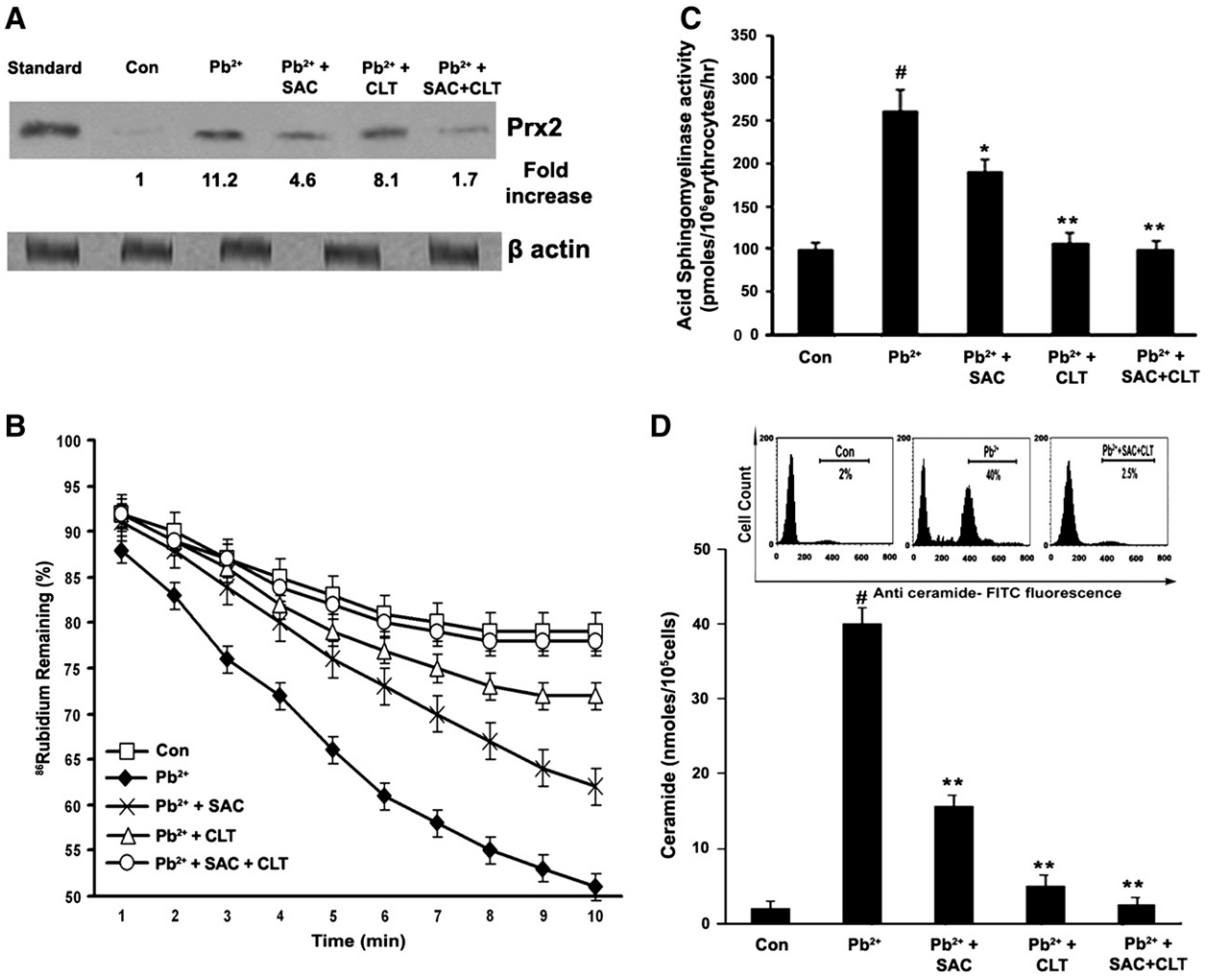

Fig. 8. SAC + CLT prevents Prx2 translocation. Gardos channel activation and ceramide generation in the erythrocytes of Pb^{2+} exposed animals. (A) Western blot analysis of translocation of Prx2 to cell membrane in the erythrocytes of Pb^{2+} exposed animals with or without SAC and CLT monotherapy and combined therapy. β-actin was used as loading control in the representative blots of three independent experiments with 6 animals in each group. (B) SAC + CLT inhibits Pb^{2+} Gardos channel activation in erythrocytes. Functioning of Gardos channel increased by Rubidium efflux assay using $^{86}Rb^{2+}$ as described under Materials and methods. Values are mean ± SD of three independent observations (n = 6). (C) Inactivation of aSMase activity in Pb^{2+} exposed animals in response to SAC + CLT treatment. aSMase activity was evaluated from the fluorescence of resorufin as described under Materials and methods. Results represent mean ± SD of three independent observations (n = 6), $^{\#}p<0.01$ vs. respective age matched control, $^{**}p<0.01$ vs. respective Pb^{2+} exposed groups. (D) SAC + CLT treatment reduces Pb^{2+} mediated increased generation of ceramide in erythrocyte. Generation of ceramide was determined cytofluorometrically using anti ceramide antibody and FITC labeled secondary antibody was described under Materials and methods. Values are mean ± SD of three independent observations (n = 6), $^{\#}p<0.01$ vs. respective age matched control, $^{**}p<0.01$ vs. respective Pb^{2+} exposed groups. Inset: representative FACS histogram of three independent observations showing inhibition of Pb^{2+} induced ceramide generation in response to combination treatment with SAC and CLT. Data were analyzed by CELL QUEST software.

also responsible for most of the hypolipidemic, antithrombotic, antioxidant and hypoglycemic effects it exerts [2]. DADS and DAS (diallyl sulfide) the active compounds of garlic are effective apoptotic agents having an anticancerous property of the cells [47]. However another active compound of garlic, a cysteine-containing agent SAC was superior to DAS and DADS in delaying glycative deterioration of plasma in non-insulin dependent diabetes [48]. Our results suggest that SAC was more potent than DADS in restoring the morphology of erythrocytes and increasing the lifespan of erythrocytes during chronic Pb^{2+} toxicity. We further aimed to clarify the differential behavior of these active compounds during Pb^{2+} toxicity by *in vitro* experiments. DADS differs from SAC only in the absence of the alanyl group (–CH_2CH–NH_2–COOH). Thus better scavenging $OH^{\bullet -}$ radicals in Pb^{2+} exposed erythrocytes by SAC than DADS could be attributed by the presence of the alanyl group in SAC [41,49].

Garlic has metal chelating ability and it is non-toxic to animals and humans at therapeutic doses [18,19]. Combination therapy with SAC and CLT did not exert any toxic effect on Pb^{2+} exposed mice. We have observed that combination therapy and monotherapy with SAC decreased Pb^{2+} concentration in blood. However, it was interesting to note that CLT monotherapy did not decrease Pb^{2+} content in blood but was capable of partially increasing the lifespan of erythrocytes. So, it is likely that there exists a diversity of mechanisms in the reduction of lifespan of erythrocytes during Pb^{2+} exposure and this might be the reason that a single target approach is less effective. The approaches to combination therapy in our study were to start monotherapy with an active substance of garlic and then followed by an addition of a second substance with a predefined treatment goal of blunting Gardos channel. Hence, combination therapy with SAC and CLT targeted a broader range of pathways than monotherapy. CLT not only prevented K^+ loss and decline in cell shrinkage of erythrocytes, it also exhibited an antioxidant property to some extent during chronic Pb^{2+} exposure to mice. CLT possesses an antiapoptotic property and also has a free radical scavenging activity [50]. SAC in combination with CLT restored the lifespan of erythrocytes to a normal level during chronic Pb^{2+} exposure. As K^+ loss is characterized by events leading to suicidal erythrocyte death, we explored these events in Pb^{2+} exposed animals treated with combination therapy.

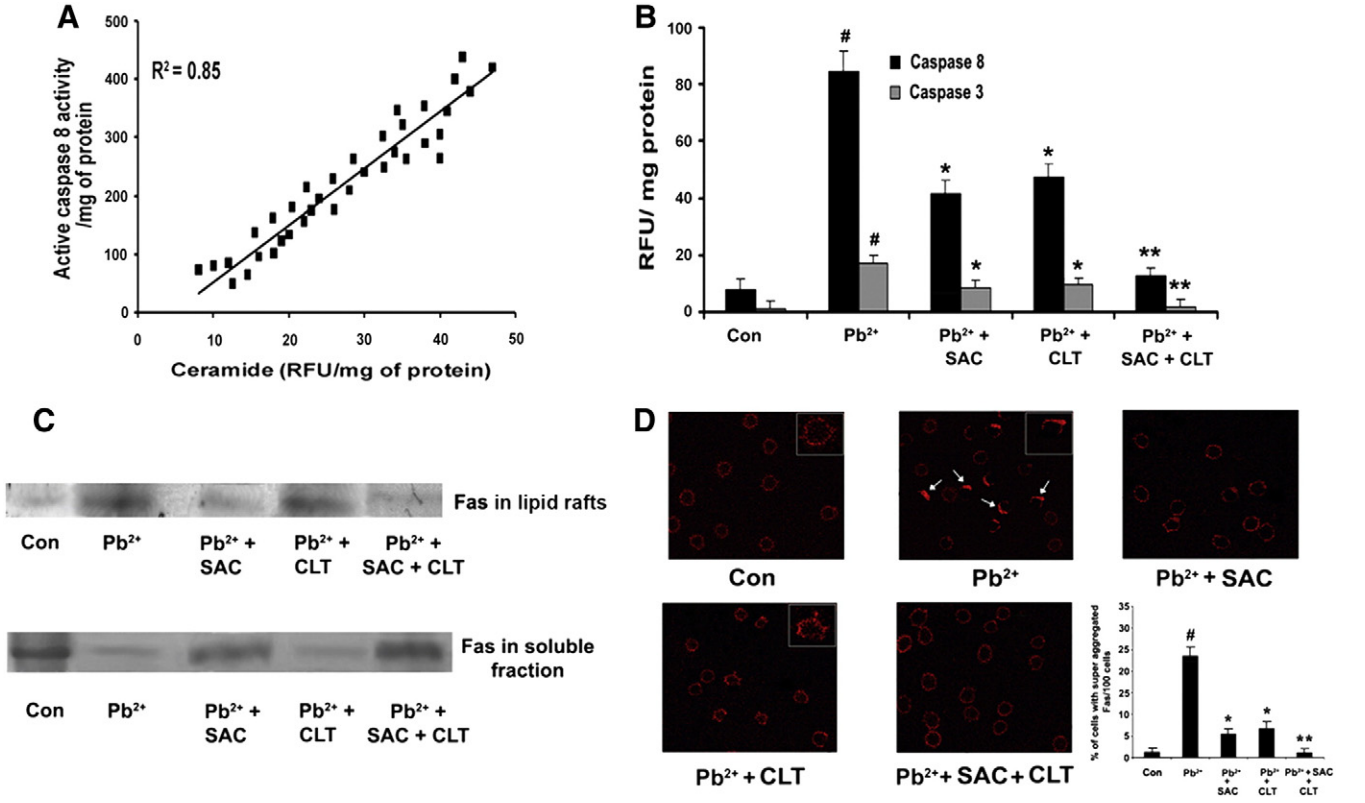

Fig. 9. SAC + CLT prevents Fas mediated apoptosis of red cells of Pb^{2+} exposed animals. (A) Correlation between ceramide and caspase 8 activities in erythrocytes at different periods of Pb^{2+} exposure. Ceramides were quantitatively estimated and caspase 8 activity was determined spectrofluorometrically as described under Materials and methods. Data are representative of three independent measurements (n = 6). (B) Inactivation of lead induced activation of caspase 8 and caspase 3 with SAC and CLT treatment. Caspase 3 and caspase 8 activities were determined using fluorometric substrates DEVD-AFC and IETD-AFC respectively, as determined under Materials and methods. Values are representative of three separate experiments (n = 6), $^{\#}p<0.01$ vs. respective age matched control, $^{*}p<0.05$ $^{**}p<0.01$ vs. respective Pb^{2+} exposed groups. (C) SAC + CLT interferes with the Pb^{2+} induced translocation of Fas to lipid rafts of red cell membrane. Fas were detected after translocation in the lipid raft (upper panel) and soluble fraction (lower panel) by immunoblot analysis as described under Materials and methods. Results are representative of three independent experiments with similar results (n = 6). (D) Representative confocal micrographs showing Pb^{2+} mediated Fas aggregation (indicated by arrows) in erythrocytes with or without SAC and CLT treatment. Cells were stained with anti Fas antibody and Alexa Fluor 633 tagged secondary antibody as described under Materials and methods. Results are representative of three separate experiments (n = 6). Inset: quantitative estimation of cells with super aggregated Fas in different treatment groups. Results are mean ± SD of three independent experiments (n = 6), $^{\#}p<0.01$ vs. age matched control, $^{*}p<0.01$, $^{**}p<0.001$ vs. respective Pb^{2+} exposed groups.

K^+ loss is associated with a decrease in cell volume, cell membrane blebbing and loss of cell membrane asymmetry with phosphatidylserine exposure at the cell surface [51]. Combination therapy successfully prevented redistribution of PS in plasma membrane in erythrocytes during Pb^{2+} exposure. To understand the potential mechanisms involved in the protection offered by SAC and CLT combination against cell death we explored the events that lead to premature death of erythrocytes during chronic Pb^{2+} exposure. Sustained oxidative stress is a major cause for the apoptosis and increased oxidative stress in Pb^{2+} exposed erythrocyte leads to premature erythrocyte death [5]. The erythrocytes recovered redox balance during combination therapy and this can be attributed more to the property of SAC. However, CLT also exhibited antioxidant property to some extent. The antioxidant activity shown by CLT is due to the imidazole moiety of the molecule. Both SAC and CLT acted synergistically in protecting cells from oxidative stress.

Cellular redox is controlled by GSH systems that scavenge harmful intracellular ROS [52]. Lipid hydroperoxides generated during oxidative stress undergo homolytic decomposition into α,β-unsaturated aldehydeic bifunctional electrophiles [53,31]. Bifunctional electrophiles can modify intracellular components like GSH to form adducts [54]. It is suggested that these adducts might be involved in depletion of cellular GSH during chronic Pb^{2+} exposure to mice as GSH–HNE are known to be actively transported out of the cells [31]. Decrease in the intracellular GSH led to the onset of apoptosis in HNE treated cells [31]. The hydrogen atom in the sulfhydryl (–SH) group of SAC can act as a scavenger for neutralizing free radicals [22,23]. Oral supplementation with SAC provided an alternate means of boosting intraerythrocytic GSH. GSH is the predominant antioxidant in the aqueous cytoplasm of cells [54]. GSH is synthesized from cysteine, and the availability of cysteine that controls the GSH synthesis [54]. Enhancement of erythrocyte GSH by a proglutathione drug like SAC may therefore add a therapeutic value to the combination of SAC and CLT.

We further evaluated the role of other major antioxidants, which failed to nullify the precursor of radicals. Catalase, GPx and Prx2 are the main defenses of erythrocyte against H_2O_2, the precursor of $OH^{\bullet -}$ radicals under most physiological circumstances [55]. However, inactivation of one of these defenses does not impair the erythrocytes ability to scavenge ROS because the activity of the other two gets sufficiently high to eliminate virtually all the incoming ROS. However during chronic Pb^{2+} exposure to mice all the three defenses in the erythrocytes lost their activity and failed to rescue the erythrocytes. During erythrocyte senescence GPx1 undergoes irreversible inactivation followed by Prx inactivation [56]. Some reports suggest that GPx inhibition leads to an inhibition of catalase [57]. There lies the possibility that peroxide-degrading systems are somewhat linked to one another under oxidative conditions, and inactivation of one system is related to the inactivation of a second system. Cytosolic Prx2 was inactivated during Pb^{2+} exposure to mice, either by dimerization or by overoxidation, and they were translocated to membrane. SAC monotherapy and combination therapy was better than CLT

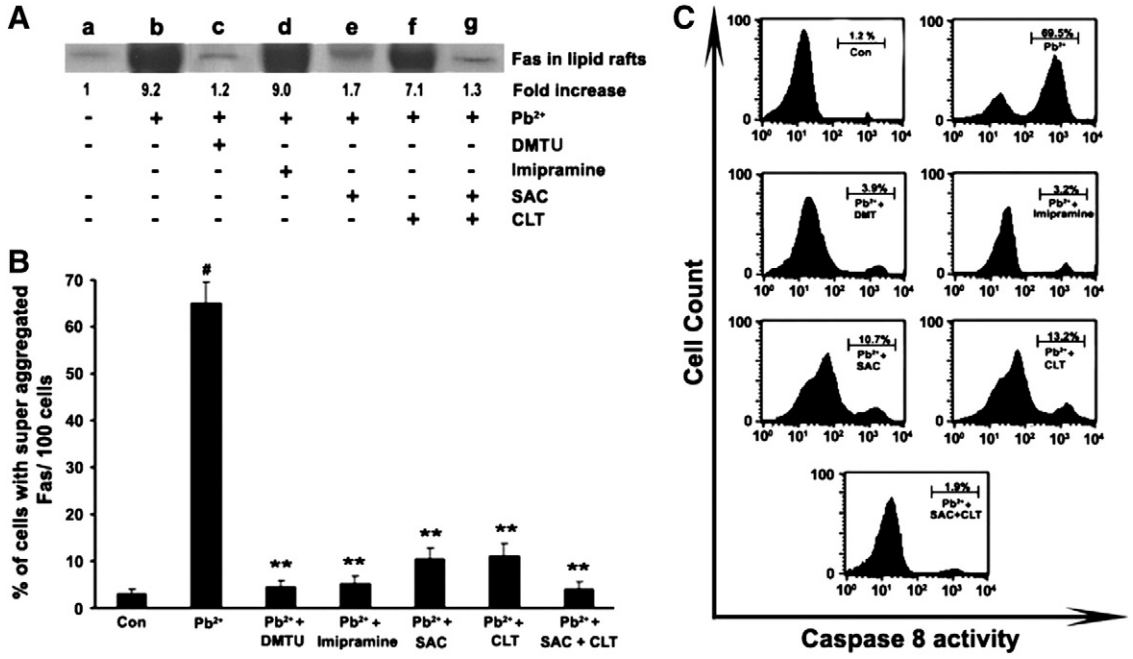

Fig. 10. Contribution of ROS and K^+ efflux on Fas mediated apoptosis of Pb^{2+} exposed erythrocytes. Erythrocytes (5×10^5) were incubated with lead acetate, (1 mM) for 9 h at 37 °C. Untreated cells served as control group. Drug treated groups were pre-incubated for 30 min with the respective drugs like SAC (0.5 mM), DADS (0.5 mM), CLT (0.1 μM), dimethyl thiourea (DMTU) (10 μM) and imipramine (100 μM) before incubation with lead acetate. Cells receiving combination treatment were incubated with 0.5 mM SAC + 0.1 μM CLT. Inhibition of ROS generation and K^+ efflux was achieved by pre-incubating with DMTU and imipramine respectively. (A) Representative western blots of Fas aggregation in lipid rafts under the indicated experimental conditions. Results are representative of three independent observations. (B) Quantitative estimation of red cells with super aggregated Fas observed under confocal microscope in different treatment groups. Cells were detected using anti Fas antibody and Alexa Fluor 633 tagged secondary antibody. Values are mean ± SD of three independent experiments, ($n=6$), $^{\#}p<0.01$ vs. respective age matched control cells and $^{**}p<0.01$ vs. respective exposed cells. (C) Representative FACS histograms of caspase 8 activity in erythrocytes from different treatment groups. Flow cytometry was done using anticaspase 8 activity and FITC tagged secondary antibody taking 1×10^5cells from different treatment groups. Results are representative of three separate experiments with similar results ($n=6$).

monotherapy in preventing translocation of Prx2 to the membrane and this could be attributed to a better antioxidant capacity of SAC than CLT. Translocation of Prx2 to the membrane certainly influences the interplay between antioxidants and peroxide-degrading systems [55]. Prx2 linkage to the membrane increases with ROS generation and occurred only when the oxidized form of the enzyme was present in the cytosol [55]. Membrane association is possibly mediated via its C-terminal extension. Prx2 binds to stomatin (band 7.2) in the membrane, which has an unusual topology with a hydrophobic domain, embedded at the cytoplasmic side of the membrane. Stomatin, a transmembrane protein regulates the activity of various membrane proteins and binding of Prx2 to stomatin may adversely influence the functions of various membrane proteins [58]. Much before its peroxidase activity was recognized, Prx2 (known also as calpromotin) was identified as a protein required by erythrocytes for Gardos channel activation [50]. Gardos channel activation plays an important role in the mechanism of cell dehydration and changes in cell morphology are associated with chronic Pb^{2+} exposure. The active influx of $^{86}Rb^{2+}$ into red cells of Pb^{2+} exposed mice decreased partially with SAC monotherapy but completely with CLT monotherapy and SAC + CLT combination therapy. The better result of CLT in preventing Gardos channel can be attributed to it by being a Gardos channel inhibitor. The presence of ceramide in Pb^{2+} exposed erythrocytes can be attributed to activation of Gardos channel. Activation of Gardos channel induces erythrocyte shrinkage that results in the activation of sphingomyelinase and increase in ceramide generation [46]. The pleotropic effects of ceramide include triggering of suicidal erythrocyte death. Reports suggest that C_6-ceramide triggers annexin binding to erythrocytes, which is not dependent on accumulated calcium in erythrocytes [59]. Ceramide accumulation was partially prevented during monotherapies and completely during combination treatment. Thus, ceramide formation probably played a permissive role in erythrocyte death during Pb^{2+} exposure. Our results suggested that translocation of Fas (CD95) receptor to lipid raft was dependent on ROS generation in cells, as SAC could prevent translocation of Fas to lipid rafts. CLT monotherapy could only partially prevented translocation of Fas into lipid rafts, indicating that ceramide was not responsible for translocation process. However, ceramide generation appeared to be correlated with the apoptotic event. Super aggregation (capping) of Fas receptors appeared to be dependent on ceramide as CLT monotherapy could not prevent translocation of Fas into lipid rafts. But it did interfere with capping of Fas. There are reports suggesting that ceramides help Fas to cap and are highly essential for formation of DISC (death inducing signaling complex) and other downstream events associated with Fas induced apoptosis [39]. Our *in vitro* results revealed that translocation of Fas to lipid raft was dependent on ROS and not on ceramides, but ceramide generation was essential for super aggregation of Fas into the lipid rafts. These results gave credence to our *in vivo* studies and explained why both SAC and CLT inhibited downstream events of Fas signaling. Drugs in combination affecting more than one target in cell during pathophysiological condition are likely to be more effective. SAC and CLT seem to have this attribute. Both these drugs acted synergistically and enhanced the lifespan of erythrocytes during Pb^{2+} toxicosis.

Acknowledgements

The authors are grateful to Prof. Siddhartha Roy, Director, IICB, Kolkata and Dr. Tapan Kumar Mishra, Principal, Vidyasagar College, Kolkata for providing infrastructural facilities. The authors are also deeply grateful to Mr. Diptendu Bhattacharyya for mass spectroscopy studies. The authors thank Mrs. Banasri Das for helping in confocal imaging studies. The authors are thankful to Mr. Prantik Ghosh, of Zoology Department, Vidyasagar College, for his active cooperation and keen interest in this work.

Reference

[1] H.A. Godwin, The biological chemistry of lead, Curr. Opin. Chem. Biol. 5 (2001) 223–227.
[2] L. Patrick, Lead toxicity, a review of the literature. Part I: Exposure, evaluation, and treatment, Altern. Med. Rev. 11 (2006) 2–22.
[3] Agency for Toxic Substances, Disease Registry (ATSDR), Toxicoloical Profile for Lead, Public Health Service, Atlanta, GA, 2007.
[4] A. Gupta, G.S. Shukla, Enzymatic antioxidants in erythrocytes following heavy metal exposure: possible role in early diagnosis of poisoning, Bull. Environ. Contam. Toxicol. 58 (1997) 198–205.
[5] O.P. Kulish, Erythropoiesis and erythropoietic activity of the blood plasma in lead anemia, Bull. Exp. Biol. Med. 75 (1973) 631–633.
[6] M. Suwalsky, F. Villena, B. Norris, Y.F. Cuevas, C.P. Sotomayor, P. Zatta, Effects of lead on the human erythrocyte membrane and molecular models, J. Inorg. Biochem. 97 (2003) 308–313.
[7] S.J.S. Flora, M. Pande, G.M. Kannan, A. Mehta, Lead induced oxidative stress and it's recovery following co-administration of melatonin or n-acetylcysteine during chelation with succimer in male rats, Cell. Mol. Biol. 50 (2004) 543–551.
[8] N. Ercal, H.G. Orhan, N.A. Burns, Toxic metals and oxidative stress part-I: mechanism involved in metal induced oxidative damage, Curr. Top. Med. Chem. 1 (2001) 529–539.
[9] D.S. Kempe, P.A. Lang, K. Eisele, B.A. Klarl, T. Wieder, S.M. Huber, C. Duranton, F. Lang, Stimulation of erythrocyte phosphatidylserine exposure by lead ions, Am. J. Physiol. Cell Physiol. 288 (2005) 396–402.
[10] E. Weiss, D.C. Rees, J.S. Gibson, Role of calcium in phosphatidylserine externalisation in red blood cells from sickle cell patients, Anemia 2011 (2010) 1–8.
[11] D. Mandal, A. Mazumder, P. Das, M. Kundu, J. Basu, Fas-, caspase 8-, and caspase 3-dependent signaling regulates the activity of the aminophospholipid translocase and phosphatedylserine externalization in human erythrocytes, J. Biol. Chem. 280 (2005) 39460–39467.
[12] D. Biswas, G. Sen, A. Sarkar, T. Biswas, Atorvastatin acts synergistically with N-acetyl cysteine to provide therapeutic advantage against Fas-activated erythrocyte apoptosis during chronic arsenic exposure in rats, Toxicol. Appl. Pharmacol. 250 (2011) 39–53.
[13] E. Friedheim, J.H. Graziano, D. Popovac, D. Dragovic, B. Kaul, Treatment of lead poisoning by 2,3-dimercaptosuccinic acid, Lancet 2 (1978) 1234–1236.
[14] G. Saxena, S.J.S. Flora, Induced oxidative stress and hematological alterations and their response to combined administration of calcium disodium EDTA with a thiol chelator in rats, J. Biochem. Mol. Toxicol. 18 (2004) 221–233.
[15] Y. Liao, J. Zhang, Y. Jin, C. Lu, G. Li, F. Yu, X. Zhi, L. An, J. Yang, Therapeutic potentials of combined use of DMSA with calcium and ascorbic acid in the treatment of mild to moderately lead intoxicated mice, Biometals 21 (2008) 1–8.
[16] K. Kalia, S.J.S. Flora, Strategies for safe and effective therapeutic measures for chronic arsenic and lead poisoning, J. Occup. Health 47 (2005) 1–21.
[17] L. Patrick, Lead toxicity part II: the role of free radical damage and the use of antioxidants in the pathology and treatment of lead toxicity, Altern. Med. Rev. 11 (2006) 114–127.
[18] C.W. Cha, A study on the effect of garlic to the heavy metal poisoning of rat, J. Korean Med. Sci. 4 (1987) 213–224.
[19] J.P. Chaverrí, M.G. Ortiz, G. Albarrán, L.B. Esparza, M. Menjívar, O.N.M. Campos, Garlic's ability to prevent in vitro Cu2+-induced lipoprotein oxidation human serum is preserved in heated garlic: effect unrelated to Cu2+-chelation, Nutr. J. 3 (2004) 1–11.
[20] N. Ercal, H.G. Orhan, N.A. Burns, Toxic metals and oxidative streess part-I: mechanism involved in metal induced oxidative damage, Curr. Top. Med. Chem. 1 (2001) 529–539.
[21] C.W. Cha, A study on the effect of garlic to the heavy metal poisoning of rat, J. Korean Med. Sci. 2 (1987) 213–224.
[22] E. Block, The chemistry of garlic and onions, Sci. Am. 252 (1985) 114–119.
[23] C.C. Ou, S.M. Tsao, M.C. Lin, M.C. Ya, Protective action on human LDL against oxidation and glycation by four organosulfur compounds derived from garlic, Lipids 38 (2003) 219–224.
[24] D. Biswas, M. Banerjee, G. Sen, J.K. Das, A. Banerjee, Mechanism of erythrocyte death in human population exposed to arsenic through drinking water, Toxicol. Appl. Pharmacol. 230 (2008) 57–66.
[25] C.C. Foreback, J. Chu, Measurement of lead in drinking water by atomic absorption spectrometry with dithizone extraction, Toxicol. Environ. Chem. 63 (1997) 163–170.
[26] D.A. Sutherland, M.S. McCall, The measurement of the survival of human erythrocytes by in vivo tagging with Cr51, Blood 10 (1955) 646–649.
[27] G. Sen, D. Biswas, M. Ray, T. Biswas, Albumin–quercetin combination offers a therapeutic advantage in the prevention of reduced survival of erythrocytes in visceral leishmaniasis, Blood Cells Mol. Dis. 39 (2007) 245–254.
[28] J.P. Nicolay, G. Liebig, O.M. Niemoeller, S. Koka, M. Ghashghaeinia, T. Wieder, J. Haendeler, R. Busse, F. Lang, Inhibition of suicidal erythrocyte death by nitricoxide, Eur. J. Physiol. 456 (2008) 293–305.
[29] R. Franco, M.I. Panayiotidis, J.A. Cidlowski, Glutathione depletion is necessary for apoptosis in lymphoid cells independent of reactive species formation, J. Biol. Chem. 282 (2007) 30452–30465.
[30] F. Tietze, Enzymatic method for quantitative determination of nanogram amounts of total and oxidized glutathione applications to mammalian blood and other tissues, Anal. Biochem. 27 (1969) 502–522.
[31] D. Biswas, G. Sen, T. Biswas, Reduced cellular redox status induces 4-hydroxynonenal-mediated caspase 3 activation leading to erythrocyte death during chronic arsenic exposure in rats, Toxicol. Appl. Pharmacol. 244 (2010) 315–327.
[32] J.T. Dodge, C. Mitchell, D.J. Hanahan, The preparation and chemical characteristics of hemoglobin free ghosts of human erythrocytes, Arch. Biochem. Biophys. 100 (1963) 119–130.
[33] J.A. Buege, S.D. Aust, Microsomal lipid peroxidation, Meth. Enzymol. 52 (1978) 302–310.
[34] J.K. Mills, H.M. Jacobs, L.S. Lessin, Assessment of the hydration state of sickle cells by phthalate ester density distribution, J. Lab. Clin. Med. 109 (1987) 486–494.
[35] D. Wolff, X. Cecchi, A. Spalvins, M. Canessa, Charybdotoxin blocks with high affinity the Ca-activated K+ channel of Hb A and Hb S red cells: individual differences in the number of channels, J. Membr. Biol. 106 (1988) 243–252.
[36] K.D. Chowdhury, G. Sen, A. Sarkar, T. Biswas, Role of endothelial dysfunction in modulating the plasma redox homeostasis in visceral leishmaniasis, Biochim. Biophys. Acta 1810 (2011) 652–665.
[37] I. Petrache, V. Natarajan, L. Zhen, T.R. Medler, A.T. Richter, C. Cho, W.C. Hubbard, E.V. Berdyshev, R.M. Tuder, Ceramide up regulation causes pulmonary cell apoptosis and emphysema-like disease in mice, Nat. Med. 11 (2005) 491–498.
[38] J.R. Muppidi, R.M. Siegel, Ligand-independent redistribution of Fas (CD95) into lipid rafts mediates clonotypic T cell death, Nat. Immunol. 5 (2004) 182–189.
[39] A. Cremesti, F.O. Paris, H. Grassme, N. Holler, J. Tschopp, Z. Fuksi, E. Gulbins, R. Kolesnick, Ceramide enables Fas to cap and kill, J. Biol. Chem. 276 (2001) 23954–23961.
[40] R.L. Argu, E. Garcia, O.N. Medina-Campos, N. Perez-Hernandez, J. Pedraza Chaverri, G. Ortega-Pierres, Hypochlorous acid scavenging activities of thioallyl compounds from garlic, J. Agric. Food Chem. 58 (2010) 11226–11233.
[41] H.S. Selhi, J.M. White, The effect of lead on the red cell membrane, Postgrad. Med. J. 51 (1975) 765–769.
[42] L.E. Eriksson, H. Beving, Calcium- and lead-activated morphological changes in human erythrocytes: a spin label study of the cytoplasm, Arch. Biochem. Biophys. 303 (1993) 296–301.
[43] M. Shields, R. Grygorczyk, G.F. Fuhrmann, W. Schwarz, H. Passow, Lead-induced activation and inhibition of potassium-selective channels in the human red blood cell, Biochim. Biophys. Acta. 815 (1985) 223–232.
[44] J.H. Lee, H.S. Kang, J. Roh, Protective effects of garlic juice against embryotoxicity of methylmercuric chloride administered to pregnant fischer 344 rats, Yonsei Med. J. 40 (1999) 483–489.
[45] M. Ouarda, C. Abdenour, Evaluation of the therapeutic efficiency of raw garlic on reproduction of domestic rabbits under lead induced toxicity, Ann. Biol. Res. 2 (2011) 389–393.
[46] S.K. Senapati, S. Dey, S.K. Dwivedi, D. Swarup, Effect of garlic (*Allium sativum* L.) extract on tissue lead level in rats, J. Ethnopharmacol. 76 (2001) 229–232.
[47] O.H. Syed, U.H. Abshar, M. Nehal, Anticarcinogenic and antitumorigenic effect of garlic and factors affecting its activity, Phcog. Rev. 1 (2007) 215–221.
[48] C.N. Huang, J.S. Horng, M.C. Yin, Antioxidative and antiglycative effects of six organosulfur compounds in low-density lipoprotein and plasma, J. Agric. Food Chem. 52 (2004) 3674–3678.
[49] M.A. Babizhayev, M.C. Seguin, J. Gueynez, R.P. Evstigneeva, E.A. Ageyeva, G.A. Zheltukhinai, L-Carnosine (-alanyl-L-histidine) and carcinine f-alanylhistamine) act as natural antioxidants with hydroxyl-radical-scavenging and lipid-peroxidase activities, Biochem. J. 304 (1994) 509–516.
[50] A. Iannelli, G. de Sousa, N. Zucchini, M.C.S. Paul, J. Gugenheim, R. Rahmani, Anti-apoptotic pro-survival effect of clotrimazole in a normothermic ischemia reperfusion injury animal model, J Surg Res. 171 (2011) 101–107.
[51] J. Schneider, J.P. Nicolay, M. Foller, T. Wieder, F. Lang, Suicidal erythrocyte death following cellular K+ loss, Cell. Physiol. Biochem. 20 (2007) 35–44.
[52] S. Ueda, H. Masutani, H. Nakamura, T. Tanaka, M. Ueno, J. Yodoi, Redox control of cell death, Antioxid. Redox Signal. 4 (2002) 405–414.
[53] R. Silva, S. Boldt, V.M. Costa, H. Carmo, M. Carvalho, F. Carvalho, M. de L. Bastos, F. Lemos-Amado, F. Remião, Evaluation of GSH adducts of adrenaline in biological samples, Biomed. Chromatogr. 21 (2007) 670–679.
[54] P.M. Goss, T.M. Bray, L.E. Hagy, Regulation of hepatocyte glutathione by amino acid precursors and camp in protein-energy malnourished rats, J. Nutr. 124 (1994) 323–330.
[55] F.M. Low, M.B. Hampton, C.C. Winterbourn, Peroxiredoxin 2 and peroxide metabolism in the erythrocyte, Antioxid. Redox Signal. 10 (2008) 1621–1629.
[56] J. Schneider, J.P. Nicolay, M. Foller, T. Wieder, F. Lang, Irreversible inactivation of glutathione peroxidase 1 and reversible inactivation of peridoxins II by H_2O_2 in red blood cells, Antioxid. Redox Signal. 12 (2010) 1235–1246.
[57] O. Baud, A.E. Greene, J. Li, H. Wang, J.J. Volpe, P.A. Rosenberg, Glutathione peroxidase–catalase cooperativity is required for resistance to hydrogen peroxide by mature rat oligodendrocytes, J. Neurosci. 24 (2004) 1531–1540.
[58] F.M. Low, M.B. Hampton, C.C. Winterbourn, Peroxiredoxin 2 and peroxide metabolism in the erythrocyte, Antioxid. Redox Signal. 10 (2008) 1621–1630.
[59] P.A. Lang, O. Beringer, J.P. Nicolay, O. Amon, D.S. Kempe, T. Hermle, P. Akel, A. Attanasio, R. Schäfer, B. Friedrich, T. Risler, M. Baur, C.J. Olbricht, L.B. Zimmerhackl, P.F. Zipfel, T. Wieder, F. Lang, Suicidal death of erythrocytes in recurrent hemolytic uremic syndrome, J. Mol. Med. 84 (2006) 378–388.